

LATE CRETACEOUS PALAEOGEOGRAPHY OF NE BOHEMIAN MASSIF: DIACHRONOUS SEDIMENTARY SUCCESIONS IN THE WLEŃ GRABEN AND KRZESZÓW BRACHYSYNCLINE (SW POLAND)

Aleksander KOWALSKI ^{1,2}

¹ University of Wrocław, Institute of Geological Sciences
Department of Structural Geology and Geological Mapping
Plac Borni 9, 50-204 Wrocław, Poland
e-mail: aleksander.kowalski@uwr.edu.pl

² Polish Geological Institute – National Research Institute Lower Silesian Branch
Aleja Jaworowa 19, 50-122 Wrocław, Poland

Kowalski, A., 2021. Late Cretaceous palaeogeography of NE Bohemian Massif: diachronous sedimentary successions in the Wleń Graben and Krzeszów Brachysyncline (SW Poland). *Annales Societatis Geologorum Poloniae*, 91: 1–36.

Abstract: This paper provides a new sedimentological and palaeogeographic interpretation of the Late Cretaceous (late Cenomanian to early Coniacian) shallow-marine succession exposed in the Wleń Graben and in the Krzeszów Brachysyncline (NE Bohemian Massif, Sudetic Block). These two tectonic subunits are outliers of the North Sudetic and Intra-Sudetic synclinalia, respectively, and contain relics of the diachronous sedimentary succession of a seaway linking the Boreal and Tethyan marine provinces during the Late Cretaceous. Results of sedimentological study and facies analysis show that the late Cenomanian sedimentation within this corridor was dominated by strong *in situ* reworking of the pre-Cretaceous bedrock driven by storm waves and possibly tidal currents. In the latest Cenomanian, siliciclastic sedimentation was followed by the deposition of offshore-transition to offshore muddy calcareous facies in the Krzeszów area, while the deposition of coarse-grained siliciclastic facies continued in the Wleń area. The nearshore clastic belt in the latter area changed into a wider strait dominated by offshore sedimentation in the early Turonian, whereby the interconnected Wleń and Krzeszów passages evolved into a uniform strait of fully-marine sedimentation. In the middle Turonian, the southern part of the strait became progressively filled with coarse-grained siliciclastic material supplied from the east. At the end of the late Turonian and in the early Coniacian, the strait funnelled bi-directional tidal currents along its axis. The youngest Cretaceous strata in the Wleń area comprise erosional relics of the early Coniacian shoreface to offshore-transition deposits. The younger Cretaceous deposits are unrepresented, probably eroded during the post-Santonian(?) tectonic inversion of the Wleń–Krzeszów strait. Despite the relatively small distance between the two relic parts of the strait, the shallow-marine succession reveals distinct diachroneity on a regional scale, reflecting an interplay of eustatic changes, differential tectonic subsidence and clastic sediment supply. This paper presents the first detailed sedimentological logs from the two study areas, with new findings of fossil fauna and flora, proposes a new palaeogeographic interpretation and discusses the influence and development of the source areas for the Cretaceous Sudetic Wleń–Krzeszów marine strait at the NE fringe of the Bohemian Massif.

Key words: Sudetic epi-Variscan cover, shallow-marine palaeostrait, wave-dominated sedimentation, tidal currents, offshore transition.

Manuscript 15 May 2020, accepted 25 February 2021

INTRODUCTION

As a result of the Late Cretaceous global sea-level rise combined with the Alpine tectonism, most of the Western and Central Europe – including almost entire Bohemian Massif – were flooded by a shallow epicontinental sea (Fig. 1;

e.g., Skoček and Valečka, 1983; Ziegler, 1990; Dercourt *et al.*, 2000; Voigt *et al.*, 2008; Vejrbæk *et al.*, 2010; Wilmsen *et al.*, 2014). The maximum marine transgression was in the Cenomanian. The concurrent Alpine folding with tectonic

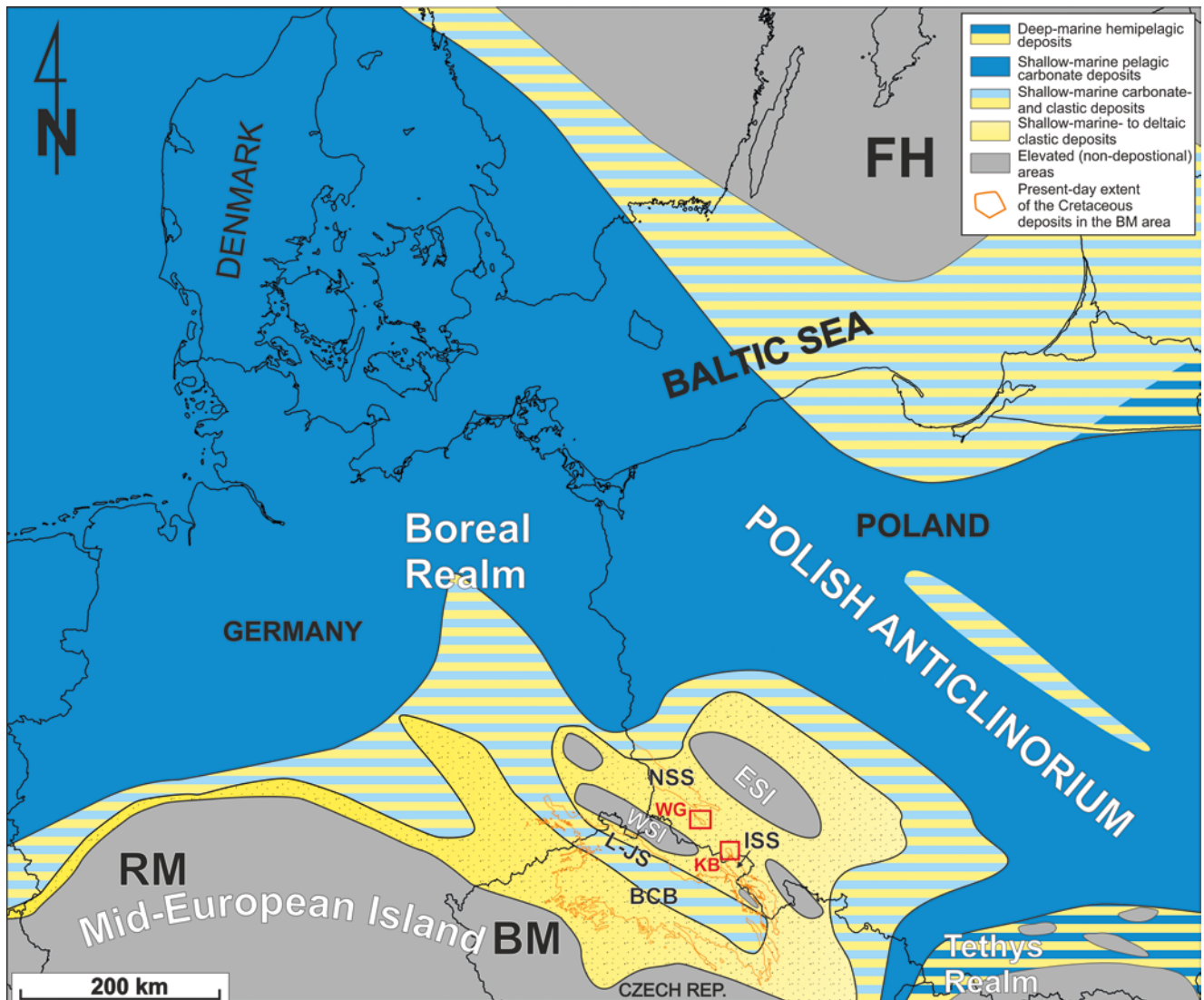


Fig. 1. Generalized facies map and extent of the Upper Cretaceous in NE Bohemian Massif and Central Europe (modified from Voigt *et al.*, 2008; Vejrbæk *et al.*, 2010; Čech, 2011; Wilmsen *et al.*, 2014). Letter symbols: BCB – Bohemian Cretaceous Basin; BM – Bohemian Massif; ESI – East Sudetic Island; FH – Fennoscandian High; ISS – Intra-Sudetic Synclinorium; KB – Krzeszów Brachysyncline; L-IS – Luzice-Jizera Subbasin; NSS – North Sudetic Synclinorium; RM – Rhenish Massif; WG – Wleń Graben; WSI – West Sudetic Island. Note the limited present-day extent of Cretaceous deposits within and around the two study areas: Wleń Graben and Krzeszów Brachysyncline (red squares).

rejuvenation of the Variscan and post-Variscan fault zones within and around the Bohemian Massif led to the formation of several successor sedimentary basins, including the North Sudetic and Intra-Sudetic basins (referred to jointly as the Sudetic basins) at the NE flank of the massif. The Late Cretaceous Sudetic basins were inherited as depocentres from a multi-stage regional development initiated by the post-Variscan tectonic extension in the Late Carboniferous that was taken over by the Late Cretaceous Alpine contraction (e.g., Nemeč *et al.*, 1982; Turnau *et al.*, 2002). The post-Variscan Sudetic basins were progressively filled with the Late Carboniferous to Middle Triassic terrestrial to shallow-marine deposits, which – after a ca. 140 Ma break in sedimentation – were discordantly covered by the Late Cretaceous marine deposits. Relics of the latter are well preserved within the North Sudetic and Intra-Sudetic

synclinoriums. A succession up to 1300 m thick of late Cenomanian–Santonian shallow marine to lacustrine-deltaic deposits occurs in the North Sudetic Basin (Milewicz, 1997; Leszczyński, 2010, 2018; Leszczyński and Nemeč, 2020), and up to 400 m thick of late Cenomanian–early Coniacian(?) shallow marine deposits in the Intra-Sudetic Basin (Wojewoda, 1997).

According to the existing palaeogeographic reconstructions, these Sudetic basins in the Late Cretaceous were semi-enclosed parts of a shallow marine passage in the peri-Tethyan shelf zone (Milewicz, 1968a, 1997), linking the Boreal North German shelf sea and the Tethyan-influenced Bohemian Cretaceous Basin (Dercourt *et al.*, 2000; Čech, 2011; Fig. 1). It is widely accepted that the Sudetic basins were interconnected and surrounded at that time by elevated landmasses (palaeo-highs): the so-called West Sudetic Island

to the west and the East Sudetic Island to the east (Partsch, 1896; Scupin, 1910, 1913, 1936; Andert, 1934; Skoček and Valečka, 1983; Milewicz, 1997; Fig. 1). These landmasses are considered to have acted as the principal source areas for siliciclastic sediment delivered to the Sudetic basins (Scupin, 1936; Milewicz, 1997; Wojewoda, 1997; Uličný, 2001; Leszczyński, 2018; Leszczyński and Nemeč, 2020). The epiplatform-type Cretaceous deposits in the Bohemian Cretaceous Basin and the Sudetic basins include distinct, basinwards-extending, thick sandstone lithosomes of littoral deposits that pass into muddy, mainly calcareous units interpreted as offshore deposits (Skoček and Valečka, 1983). The thick sandstone units were termed by German geologists in the mid-19th century as Quadersandstein (“Jointed Sandstone”), whereas the mudstone-dominated units were referred to as the Pläner (Raumer, 1819). The stacking patterns and interfingering of the two main lithological varieties were interpreted as a response to eustatic changes strongly modified by local factors: fluctuations in sediment supply from the framing massifs (“islands”) and regional Alpine tectonics (Wojewoda, 1997; Uličný, 2001; Leszczyński and Nemeč, 2020).

However, the present-day distribution of the Upper Cretaceous seems to be a combined result of the primary configuration of the Sudetic basins and their Alpine tectonic deformation. The North Sudetic Basin and Intra-Sudetic Basin were inverted by compressional and transpressional tectonics into the fault-bounded regional units trending NW–SE and known as the North Sudetic and Intra-Sudetic synclinoriums, respectively (e.g., Solecki, 1994, 2011; Żelaźniewicz *et al.*, 2011). Due to their structural fragmentation, the synclinal structures include a series of minor, adjoining subunits – synclines, grabens, half-grabens and horsts – delimited by NW–SE and NE–SW-trending regional fault systems (Fig. 2; see: Wojewoda and Mastalerz, 1989; Cymerman, 2004). Therefore, a precise palaeogeographic reconstruction of the Cretaceous Sudetic basins is not an easy task, as must take into account their isolated structural outliers. The most distinct of these outlier subunits are the Wleń Graben (WG) and the Krzeszów Brachysyncline (KB) located at the termini of the North Sudetic and Intra-Sudetic synclinoriums, respectively (Fig. 2). They are the subject of the present study as integral structural relics of the hypothetical Sudetic gateway between the Boreal and Tethys provinces (Fig. 1). The WG and KB are ca. 40 km apart, separated by crystalline basement structures devoid of post-Variscan sedimentary cover (Fig. 2), but are the potential regional clue as to the hypothetical interconnection of the North Sudetic and Intra-Sudetic basins (Scupin, 1936; Milewicz, 1997; Wojewoda, 1997; Voigt *et al.*, 2008; Leszczyński, 2018).

The Late Cretaceous sedimentary successions of the Sudetic basins were extensively studied, but the basinal outliers peripheral to the North Sudetic and Intra-Sudetic synclinoriums remained little analysed in terms of their sedimentary facies details and regional palaeogeographic significance (Jerzykiewicz, 1971; Gorczyca-Skała, 1977). Palaeocurrent directions measured by Jerzykiewicz (1968) in the Upper Jointed Sandstone unit (uppermost Cretaceous) in the KB remained uncomparated to those in

the North Sudetic Synclinorium. Some selected aspects of the Upper Cretaceous in the KB were considered in more recent conference reports (Wojewoda, 1998a, b, c; Kowalski, 2016), but no comprehensive sedimentological study of these deposits was conducted, whereas the Cretaceous in the WG remained virtually unstudied. Some general regional descriptions linked to the Detailed Geological Map of the Sudetes at a scale of 1:25 000 were published (Don *et al.*, 1981b; Milewicz and Frąckiewicz, 1988; Szałamacha and Szałamacha, 1993b), but the resolution of these maps and their applicability in palaeogeographic considerations is relatively low (cf. Cymerman, 2016; Wojewoda, 2016). No detailed sedimentological logs and comparative analysis of the Cretaceous deposits in their individual outcrops have thus far been published, although numerous borehole data became recently available (e.g., Wojtkowiak *et al.*, 2009; SPDPSH, 2019).

The primary objective of this study is to resolve discrepancies and improve the understanding of the Late Cretaceous palaeogeography in the peripheral parts of the North Sudetic and Intra-Sudetic synclinoriums based on integrated outcrop-scale sedimentological studies, facies analysis, new borehole data, and enhanced geological mapping. A repetition of cartographic survey with the use of digital field techniques was the key starting point for further sedimentological studies. The present report is the first attempt of detailed lithostratigraphic correlation, presentation of the spatial distribution of sedimentary facies and a comparative analysis of the Upper Cretaceous in the WG and KB, including palaeocurrent measurements and borehole data. Presented are also some remarks and considerations in relation to the new findings of fossil fauna, bioturbation structures and flora remains, although detailed palaeontological and ichnological studies are beyond the scope of this paper. A comprehensive stratigraphic scheme for the Upper Cretaceous in the KB and WG is proposed, with an interpretive review of the Late Cretaceous palaeogeographic evolution in these areas based on palaeotransport indicators.

GEOLOGICAL SETTING AND STRATIGRAPHIC FRAMEWORK

The WG and KB are tectonic subunits located in the peripheral parts of the North Sudetic and Intra-Sudetic synclinoriums, respectively (Fig. 2), with a partly preserved Cretaceous shallow-marine sedimentary succession. The base of the marine Upper Cretaceous is a major regional unconformity that separates these deposits from the older, post-Variscan sedimentary rocks or Variscan metamorphic units (Figs 2, 3). In the KB, the Cretaceous deposits overlie unconformably a faulted and lithologically differentiated bedrock (Fig. 3) composed of the terrigenous clastic Lower Triassic (Buntsandstein) and Lower Permian (Rotliegend). In the WG, the Cretaceous discordantly overlaps in the NW–SE direction the Buntsandstein and Rotliegend as well as the Cambrian to Early Carboniferous metamorphic rocks of the Kaczawa Metamorphic Complex (cf. Baranowski *et al.*, 1990). The study areas are separated from each other at a distance of ca. 40 km by crystalline rocks of the Karkonosze

Granitic Massif, Eastern Karkonosze Metamorphic Unit and Kaczawa Metamorphic Complex (Fig. 2).

The SE-trending Wleń Graben (WG) is a SE outlier of the North Sudetic Synclinorium and constitutes a well-developed, ca. 17.5 km long and up to 3.5 km wide tectonic trough bounded by steep normal and reverse faults (Kolb, 1936; Milewicz, 1959; Gorczyca-Skała, 1977; Gierwielaniec, 1998; Kowalski, 2020b). The bedrock and elevated flanks of the graben consist predominantly of the epi-metamorphic rocks of Kaczawa Metamorphic Complex, whilst the graben interior is composed of the late Carboniferous to Early

Permian (Rotliegend) terrigenous clastics, Late Permian (Zechstein) marine strata, Early Triassic (Buntsandstein) terrigenous deposits, and their Late Cretaceous shallow-marine cover. The present paper follows the lithostratigraphic scheme for sedimentary succession of the North Sudetic Synclinorium proposed by Milewicz (1985).

The undivided Upper Carboniferous to Lower Permian in the northern and central parts of the WG (the Świerzawa Formation of Milewicz, 1965, 1985; Śliwiński *et al.*, 2003) consist of poorly sorted, coarse-grained clastics representing alluvial fan and pebbly braided river deposits (Kowalski

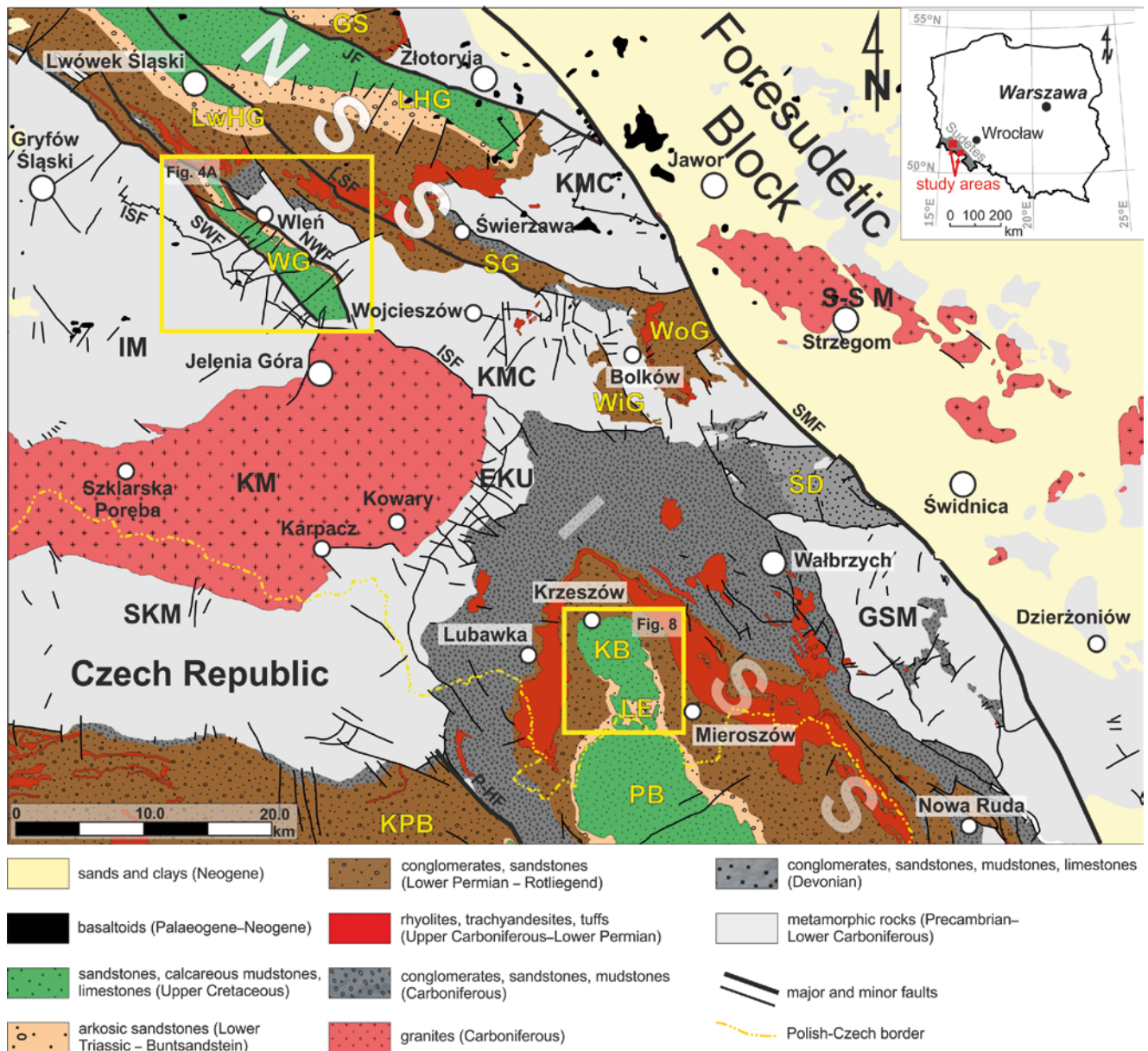


Fig. 2. Simplified geological map of the marginal parts of the North Sudetic Synclinorium (NSS) and Intra-Sudetic Synclinorium (ISS) with location of detailed geological maps presented in Figs 4A and 8 (yellow squares). Letter symbols: GS – Grodziec Syncline; KPB – Karkonosze Piedmont Basin; LHG – Leszczyna Half-Graben; LwHG – Lwówek Śląski Half-Graben; ŚD – Świebodzice Depression; ŚG – Świerzawa Graben; WiG – Wierzchosławice Graben; WoG – Wolbromek Graben; WG – Wleń Graben; EKU – Eastern Karkonosze Unit; GSM – Góry Sowie Massif; IM – Iżera Massif; KM – Karkonosze Massif; KMC – Kaczawa Metamorphic Complex; SKM – South Karkonosze Metamorphic Unit; S-SM – Strzegom-Sobótka Massif; IF – Intrasudetic Fault; JF – Jerzmanice Fault; LŚF – Lwówek-Świerzawa Fault; NWF – Northern Wleń Fault; SWF – Southern Wleń Fault; P-HF – Połiči-Hronov Fault; SMF – Sudetic Marginal Fault. Geological map based on Sawicki (1995) and Cymerman (2004).

et al., 2018). They are cut by shallow sub-volcanic bodies, lava flows and dykes of trachyandesites, trachybasalts and rhyolitoids (the “Lower Permian Volcanic Complex” of Milewicz, 1965; Kozłowski and Parachoniak, 1967; Awdankiewicz, 2006) capped by fluvial sandstones and conglomerates with calcrete-type cementation (the Bolesławiec Formation of Milewicz, 1985; Raczyński, 1997; Raczyński *et al.*, 1998; Śliwiński *et al.*, 2003). The thickness of Rotliegend in the North Sudetic Synclinorium is estimated at ca. 1300 m (cf. Milewicz, 1965). The Rotliegend succession is unconformably covered by the marine Upper Permian represented by dolomites of the third Zechstein cyclothem (PZ3, <15 m thick; Milewicz, 1966; Kowalski *et al.*, 2018), grading into mudstones and fine-grained sandstones assigned to the Permo-Triassic Transitional Terrigenous Series (PZt; Peryt, 1978) interpreted as deposits of a muddy coastal plain formed during the Zechstein Sea regression. Zechstein deposits reach a thickness of 10 to 30 m and pass upwards nearly concordantly into sandstones and conglomerates assigned to the Buntsandstein of the Radłówka Formation (Scupin, 1933; Milewicz, 1968b; Mroczkowski, 1969, 1972; Kowalski, 2020a), considered to represent fluvial sedimentation (Mroczkowski, 1969, 1972; Mroczkowski and Mader, 1985; Kowalski, 2020a). The Lower Triassic reaches a thickness of 340 m in the northern part of the WG (Kowalski, 2020a).

The Late Cretaceous (late Cenomanian to early Coniacian?) marine deposits, forming the main structure of the WG, are distinguished therein and in the entire North Sudetic Synclinorium as the Rakowice Wielkie Formation (Milewicz, 1985, 1997). The Cretaceous succession in the WG begins with the “basal (transgressive) conglomerate” linked to the main, late Cenomanian marine invasion (Gorzycza-Skała, 1977). The conglomerates form a 0.1–1 m thick, discontinuous bed passing upwards into a thick,

glauconitic-siliceous and locally calcareous sandstones (the “Lower Jointed Sandstone”; Fig. 3), distinguished in the North Sudetic Synclinorium as the Wilków Member (upper Cenomanian; Milewicz, 1997). In the uppermost part of, the glauconitic sandstones pass into arkosic and subarkosic varieties. The Wilków Member in the WG area has a thickness of ca. 37 m (boreholes Łupki-4 and Czernica-1; SPDPSH, 2019), decreasing to ca. 22 m to the south (borehole Płoszczyna-1; SPDPSH, 2019). The Wilków Member sandstones are covered by a monotonous succession of calcareous mudstones, siltstones and marl/limestone alternations referred to herein as the Heterolithic Series (Fig. 3), reaching a thickness of ca. 280–300 m in the central part of the WG (borehole Nielestno-3; SPDPSH, 2019). Based on the findings of bivalves, including *Inoceramus subcardisoides soukoui* Mitura in their uppermost part (Gorzycza-Skała, 1977), the Heterolithic Series deposits are assigned to the Turonian and possibly early Coniacian. The Middle Jointed Sandstone assigned in other parts of the North Sudetic Synclinorium to the Chmielno Member (Milewicz, 1997) do not occur in the WG. At two isolated localities (the Gniazdo and Stromiec hills) in the central part of the WG, the Heterolithic Series deposits are capped by massive, coarse-grained quartzose and locally arkosic sandstones (Upper Jointed Sandstone) distinguished as the Żerkowice Member (cf. Milewicz, 1997). The youngest Cretaceous deposits, assigned in the North Sudetic Synclinorium area to the Węgliniec and Czerna formations (upper Coniacian–Santonian), do not occur in the WG. The most complete, up to 450 m thick Cretaceous marine succession is preserved in the central part of the WG. The volcanoclastic rocks of the WG are cut by Palaeogene and probably Neogene basaltoids (Milewicz and Frąckiewicz, 1983; Badura *et al.*, 2006). Quaternary deposits in the WG area attain a thickness of up to 20 m (Milewicz and Frąckiewicz, 1983, 1988).

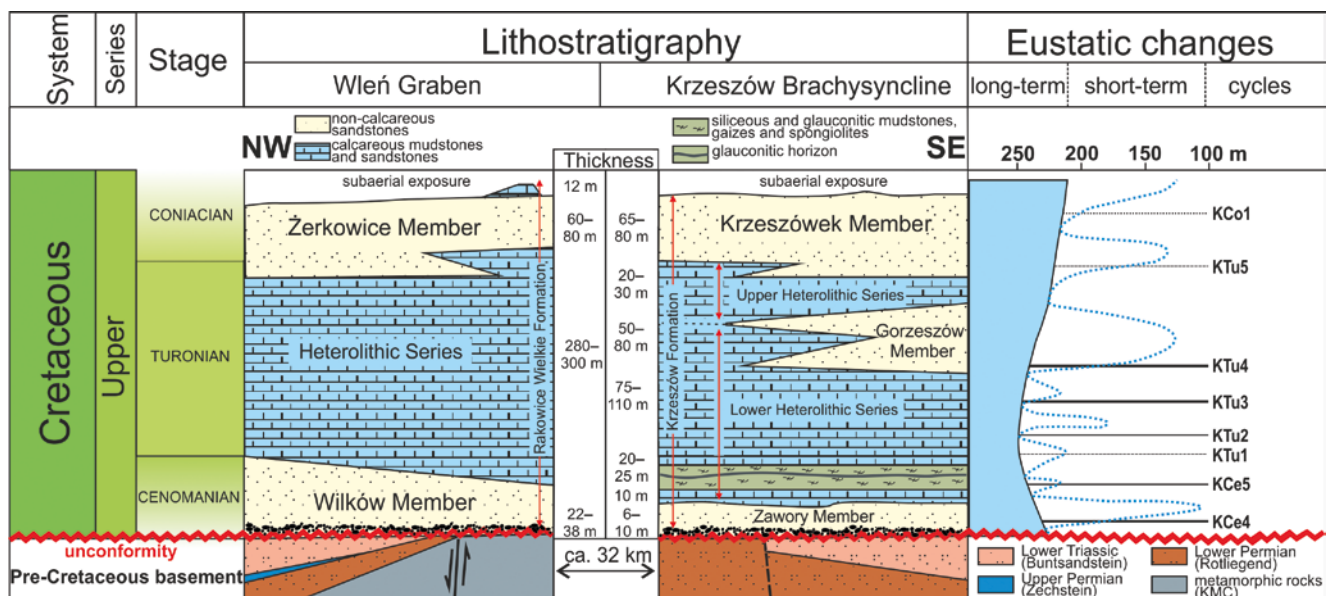


Fig. 3. Synthetic stratigraphic scheme of the Upper Cretaceous in the Wleń Graben and Krzeszów Brachysyncline, presented in a NW–SE axial cross-section through these units. The lithostratigraphic scheme for the WG is based on Milewicz (1997); the lithostratigraphy for the KB is as proposed herein. The eustatic curves (with long- and short-term sea-level changes indicated by solid and dotted blue curves, respectively) are based on Haq (2014).

The Krzeszów Brachysyncline (KB), as a NE structural outlier of the Intra-Sudetic Synclinorium, sits unconformably atop the Kamienna Góra Syncline (cf. Cymerman, 2004), which is composed mainly of the upper Carboniferous to lower Permian volcanoclastic rocks. The sedimentary succession building the main structure of the KB encompasses Lower Permian (Rotliegend) to Lower Triassic (Buntsandstein) clastics, which are discordantly overlain by the Upper Cretaceous (upper Cenomanian to upper Turonian/lower Coniacian?) shallow-marine strata (cf. Jerzykiewicz, 1971; Wojewoda, 1998a). Due to the lack of a consistent stratigraphic scheme for the northernmost part of the Intra-Sudetic Synclinorium, a basic lithostratigraphic subdivision of the Upper Cretaceous in the KB is proposed in this paper (Fig. 3), partly corresponding to that used by early German geologists (cf. Flegel, 1904; Scupin, 1935).

The Rotliegend deposits, assigned to the Chełmsko Śląskie Beds (Dziedzic, 1961; Śliwiński, 1980, 1981, 1984), occur in the marginal parts of the KB and consist of coarse-grained clastics with calcareous intercalations, interpreted as alluvial fan and braided river deposits with caliche and travertine horizons. The bulk thickness of the Chełmsko Śląskie Beds reaches 45 m. They are unconformably overlain by the Buntsandstein, assigned to the Bohdašin Formation in the Czech part of the Intra-Sudetic Synclinorium (Tásler, 1964) and reaching a thickness of 150 m in the KB area (Kowalski 2020a). The Buntsandstein is interpreted as braided river deposits (Mroczkowski, 1977; Mroczkowski and Mader, 1985; Prouza *et al.*, 1985; Kowalski, 2020a) and is overlain by the Early to Middle(?) Triassic “kaolinitic sandstones” (Kowalski, 2016, 2017, 2020a) representing a transition from fluvial to shallow lacustrine environment (Kowalski, 2020a). According to other researchers, the kaolinitic sandstones represent shallow-marine (Wojewoda *et al.*, 2016), lacustrine (Prouza *et al.*, 1985) or even aeolian deposits (Uličný, 2004).

The Cretaceous marine deposits overlie Buntsandstein in the southern and central parts of the KB (Kowalski, 2020a) and Rotliegend conglomerates in its northern part (Jerzykiewicz, 1971). The name Krzeszów Formation is proposed for the entire Cretaceous succession exposed in the KB area. The boundary between the Krzeszów Formation and older deposits is marked by the “basal (transgressive) conglomerate” that covers a nearly horizontal, regional transgressive unconformity (Fig. 3) and passes upwards into quartzose and glauconitic sandstones (the Lower Jointed Sandstone), up to 10 m thick, referred to herein as the Zawory Member (Fig. 3) and known as the Peruc-Koryčany Formation (Čech *et al.*, 1980) in the Czech part of the Intra-Sudetic Synclinorium. The glauconitic sandstones pass upwards into calcareous sandstones, up to 15 m thick, which grade into glauconitic and siliceous mudstones with spongiolitic intercalations, considered to be of a late Cenomanian (Jerzykiewicz, 1971; Teisseyre, 1972) to early Turonian age (the Bílá Hora Formation; Čech *et al.*, 1980). Within the mudstones occurs the “glauconite horizon” of Berg and Dathe (1940). The siliceous mudstones pass upwards into the middle to late Turonian calcareous mudstones, exposed in the central part of the KB (Jerzykiewicz, 1971; Don *et al.*, 1981a) and referred to in the present paper

as the Lower and Upper Heterolithic series (Fig. 3). These are separated by a distinct unit, up to 80 m thick, of arkosic and subarkosic sandstones (the Middle Jointed Sandstone; Jerzykiewicz, 1971) assigned to the Jízerka Formation in the Czech part of the Intra-Sudetic Synclinorium (Čech *et al.*, 1980). The term Gorzeszów Member is proposed herein for these sandy deposits in the KG (Fig. 3). The Upper Heterolithic Series, above the Gorzeszów Sandstone Member, is capped by a non-calcareous sandy lithosome – the Upper Jointed Sandstone (Jerzykiewicz, 1968), known as the Teplice Formation (Čech *et al.*, 1980) in the Czech part of the Intra-Sudetic Synclinorium and referred to herein as the Krzeszówek Member (cf. Fig. 3). Due to the lack of diagnostic fauna, their age is only roughly estimated as the late Turonian–early Coniacian (Jerzykiewicz, 1968, 1971; Wojewoda, 1998a, c). The top of these sandstones is erosional and they are the youngest preserved Cretaceous deposits in the Intra-Sudetic Synclinorium. The bulk thickness of the Cretaceous marine clastic deposits in the KB area reaches 350 m (Jerzykiewicz, 1971).

METHODS

Conventional and digital field techniques and laboratory methods were used. The starting part of sedimentological studies included a geological mapping survey at a scale of 1 : 10 000 as well as an analysis of available borehole data, both conducted in 2015–2020. Borehole profiles with documented substantial thickness of the Upper Cretaceous were analysed (5 boreholes in the WG and 8 boreholes in the KB). Although some of the historical borehole data could not be fully utilised due to missing cores, information from archive databases (SPDPSH, 2019) and sedimentary-hydrogeological documentations (e.g., Wojtkowiak *et al.*, 2011) was applied. Mapping surveys included surface observations in both natural and artificial outcrops, such as tors, abandoned or periodically active quarries and road crosscuts. The studied sites were localised with the use of GPS receivers with an accuracy of position determination from 1 to 3 m. The mapped area encompassed ca. 55 km² in the WG and 60 km² in the KB with its nearest proximities. Geological maps were constructed with the application of high-resolution, LiDAR-based (Light Detection and Ranging) Digital Elevation Models (DEMs) with a primary resolution of 1 × 1 m, obtained from the Polish Centre of Geodetic and Cartographic Documentation as XYZ point data grids with a density of ca 4–6 point/m² and an average elevation error not exceeding 0.3 m. These data were acquired by airborne laser scanning (ALS) performed in Poland in 2011–2014 within the frame of project ISOK (IT System of the Country’s Protection against Extreme Hazard). The DEMs helped to determine regional stratigraphic boundaries and fault surfaces, and to create intersection lines between geological bodies with the use of GIS software (Global Mapper v. 12.0, SAGA GIS v. 7.0 and Microdem Software v. 2015.8 developed by Peter Guth). Based on the resulting new geological maps presented in this paper and the author’s earlier publications (Kowalski, 2015, 2017, 2018, 2020a, b), a regional stratigraphic and lithological correlation of the Cretaceous succession in both study areas was achieved.

After the geological mapping and selection of the most representative sites, conventional field and laboratory sedimentological studies were performed. A total of 783 exposures of Cretaceous deposits were studied, and were grouped into 37 representative sites for the purpose of this paper. Sedimentological studies of outcrops included macroscopic recognition, description, classification and detailed characterization of beds, as well as vertical logging of the rock texture and sedimentary structures. The individual sedimentary units were labelled with the use of standard lithofacies codes (Miall, 1978, 1985; Zieliński and Pisarska-Jamrózy, 2012). Special attention was given to the geometry, arrangement and stacking pattern of sedimentary units, including their lateral and vertical variation. The lithofacies distinguished (Table 1) served for the interpretation of sedimentary processes and palaeoenvironmental reconstruction. The study included also recognition and description of macro- and ichnofossils, examined mainly in oblique or vertical cross-sections or within loosely scattered blocks. Special attention was given to bioturbation intensity and style, as well as the distribution and preservation of macrofossils.

Palaeocurrent direction data were obtained from the main indicators, such as planar and trough cross-stratification in sandstones. Orientation of these structures was plotted as rose diagrams, taking into account the tectonic tilt of the strata. The mean and maximum particle sizes (MPS) of the individual sedimentary units were recorded. Additionally, the orientation of clast longest axes and imbrication within transgressive basal conglomerates were measured (cf. Potter and Pettijohn, 1963; Adamovič, 1994). Macroscopic descriptions of sedimentary units were supplemented with petrographic optical microscope observations. For selected main lithological types, a total of 105 thin sections were made and investigated with the use of a Nikon Eclipse LV100N POL polarizing microscope. Basic grain and matrix parameters were established with the use of ImageJ software.

STUDY RESULTS

The Upper Cretaceous occupies large parts of the WG and KB structural units. In these two mapped areas, the outcrops of Cretaceous rocks cover an area of 34.98 km² in the KB and 28.01 km² in the WG.

Upper Cretaceous in the Wleń Graben

Spatial extent, tectonics and stratigraphy

The Upper Cretaceous, assigned to the Rakowice Wielkie Formation (Milewicz, 1985), occurs throughout the Wleń Graben main structure within a series of minor, adjoining, fault-bounded grabens, half-grabens and horsts (Fig. 4A; Kolb, 1936; Gorczyca-Skała, 1977; Kowalski, 2020b). They include, from the NW, the Golejów, Klecza, Nielestno, Grodowa, Płuszczyna, Jeżów Sudecki and Szybowcowa segments. The Cretaceous is delimited by the SE-trending boundary master faults of the WG: the Southern Wleń Fault (Gorczyca-Skała, 1977) and the Northern Wleń Fault (Gorczyca-Skała, 1977; Fig. 4A), which separate the

volcano–sedimentary succession of the WG from its elevated shoulders (Kaczawa Metamorphic Complex and the North Sudetic Synclinorium at the NE terminus of the graben; Fig. 2). The total vertical displacement along the graben bounding faults, estimated from cartographic and borehole data, is from ca. 300 m in the northern part of the WG to ca. 600 m in its southern part (Kowalski, 2020b).

To the north of the WG, the Cretaceous crops out within the asymmetrical and relatively shallow, rhomb-shaped Golejów Graben (Fig. 4A) with the Wilków Member sandstones and overlying Heterolithic Series exposed in its central part. To the south, the Golejów Graben fill is dissected by the Golejów Fault with a ca. 350 m vertical throw (Kowalski, 2020b). The latter fault together with the Łupki Fault border the Golejów Graben from the Klecza Graben (Fig. 4A). The steep opposite limbs of the Klecza Graben contain Wilków Member sandstones deformed and tilted at nearly 90° (Fig. 4A), occurring within narrow belts trending NW–SE, parallel or subparallel to the graben-bounding faults. The interior of the Klecza Graben is built of mudstones of the Heterolithic Series, which dip at low angles of up to 30° towards the graben axis. In the widest, axial part of the Klecza Graben is a morphologically uplifted block (horst?; Gniazdo Hill) built of the Coniacian Żerkowice Member sandstones. The SE terminus of the Klecza Graben is dissected by the NE-trending Bóbr faults (Fig. 4A) that constitute the boundary zone between the Klecza Graben and the Nielestno Graben. The Nielestno Graben is ca. 2 km wide and built of the Heterolithic Series in the central part and of steeply tilted to vertical Wilków Member sandstones at the graben flanks (Fig. 4A). From the NE through the Grodowa Fault, the Klecza and Nielestno grabens are adjacent to the Grodowa Horst composed mainly of Buntsandstein, locally overlain by flat-lying Wilków Member sandstones.

The southern sectors of the Wleń Graben are much wider (up to 3.5 km), with the nearly symmetrical Płuszczyna and Jeżów Sudecki grabens (Fig. 4A) bordered by the main WG bounding faults and separated by the transverse Jeżów Fault. The central part of the Płuszczyna Graben is occupied by the mudstones of Heterolithic Series capped by the Żerkowice Member sandstones forming the Stromiec Hill (551 m a.s.l.). The southern boundary of the Jeżów Sudecki Graben shows the Wilków Member sandstones, moderately tilted and N-dipping at up to 40°, resting unconformably on metamorphic rocks of the Kaczawa Metamorphic Complex. The southernmost Szybowisko Graben is a relatively deep and narrow trough (up to 100 m wide and 300 m long; Kowalski, 2020b) that contains of the Wilków Member sandstones and Heterolithic Series mudstones bounded by SSE-trending steep faults. Notably, the Szybowisko Graben has not been previously recognized in the regional literature, with the Kaczawa Metamorphic Complex marked in its place on detailed geological maps (Zimmermann, 1932; Szałamacha and Szałamacha, 1993a). Distinction of the Szybowisko Graben became possible through the new borehole Szybowisko-22B (Fig. 4A; Sroga *et al.*, 2018; Kowalski, 2020b), where up to 88 m of the Turonian mudstones of Heterolithic Series were drilled without reaching the basement rocks.

Table 1

Main lithofacies of the Upper Cretaceous in the Wleń Graben and the Krzeszów Brachysyncline.

Facies associations	Facies	Textural characteristics	Sedimentary structures and other features	Interpreted origin
Gravelly lithofacies association	Gm GSm Gm _g GSm _g	Massive or normal-graded, clast- or matrix-supported conglomerates with scattered coquina. Interbeds of massive sandstones with granules scattered in coarse sand.	Continuous or discontinuous gravel sheets resting on erosional surfaces. Common clast <i>a</i> -axis alignment parallel to flow direction. Rare bioturbation structures, including <i>Ophiomorpha</i> isp.	Tractional transport by strong, erosive wave action (transgressive lag) combined with storm-generated currents; sand bypass conditions.
	GSc SGc	Coquina beds with admixture of granules and pebbles.	Continuous, laterally extensive lags or clusters of shell debris mixed with gravel. Sharp, undulating erosional bases. Accumulations of convex-up <i>Pecten</i> -like coquinas.	Storm-derived lags formed under strong erosion and winnowing of sand-sized particles in combined-flow conditions.
Sandy/muddy lithofacies association	St, SGt	Medium to very coarse sandstone, moderately to well sorted. Local concentrations of sub- and well-rounded pebbles.	Trough cross-stratification, locally as faint relics. Pseudoimbrication of scattered pebbles resting on bedform lee side. Reactivation surfaces.	Migration of sinuous-crested, linguoid or crescentic 3D dunes, driven by unidirectional currents probably on upper shoreface.
	Sp, SGp Sp ₁	Medium to very coarse sandstone, moderately to well sorted. Local granule- and pebble-rich intercalations.	Planar cross-stratification, locally as faint relics. Pseudoimbrication of scattered pebbles resting on bedform lee side. Reactivation surfaces.	Migration of straight-crested, 2D dunes driven by unidirectional currents probably on upper shoreface. Where vertically stacked, may represent longitudinal tidal sand bars (ridges).
	Su, SFu	Fine to medium sandstone, locally with silty intercalations. Moderately to well sorted, with floating granules.	Sharp-based, lens-shaped sand beds with gently inclined or undulating vague stratification, probably of hummocky type.	Tempestites deposited by sand-laden combined-flow currents.
	Srw, Src	Fine to medium sandstone, well to very well sorted.	Wave- and current ripple cross-lamination; symmetrical and asymmetrical ripple forms observed in vertical sections.	Deposition by oscillatory or unidirectional currents above the wave-base level.
	Sm Sm _g	Medium to coarse sandstone, poorly to well sorted. Small admixture of quartz granules.	Massive or normal-graded sand beds with undulating erosional bases. Scattered body fossils, rare bioturbation structures.	Seafloor sand liquefaction by wave loading or dune collapses. Possible rapid dumping of sand from overcharged storm-driven currents.
	Sb SFb	Fine to coarse sandstone, locally with silty intercalations. Moderately sorted. Small admixture of quartz granules.	Massive sand beds rich in bioturbation structures, including <i>Ophiomorpha</i> isp., <i>Thalassinoides</i> isp. and U-shaped escape traces. Locally totally burrowed.	Intense burrowing of seafloor sand by benthic organisms, episodically interrupted by storm wave influence.
	Fm FSm	Homogenous mudstone with silty and sandy intercalations. Pillow-shaped calcareous concretions with glauconite.	Massive mudstone and sandy/silty mud beds, locally with faint planar or undulating parallel lamination.	Deposition by fine-grained sediment fallout from hypopycnal suspension plumes generated by storms or far-away coastal river outlets.
	Fb FSb	Homogenous, burrowed to strongly bioturbated mudstone with silty and sandy intercalations.	Massive mudstone with <i>Ophiomorpha</i> isp. and <i>Thalassinoides</i> isp. Local faint relics of primary lamination.	Seafloor mud intensely burrowed by benthic organisms, generally below the storm wave base.

Lithology, petrography and sedimentary facies

The Lower Jointed Sandstone (Wilków Member, upper Cenomanian). The lowermost part of the Wilków Member (Fig. 3) occurs within all structural subunits of the WG (Fig. 4A) and reaches a thickness of up to 37 m in the northern (boreholes Łupki-4 and Nielestno-3) and central sectors of the graben (borehole Czernica-2). Only in the borehole Płoszczyna-1, the sandstones attain a minimum thickness of ca. 22 m (SPDPSH, 2019).

The lowermost part of the Wilków Member in most cases consists of well sorted, yellowish-grey to greyish-green, clast-supported and mainly monomictic quartz conglomerates that correspond to the transgressive “basal conglomerate” unconformably overlying the pre-Cretaceous bedrock (Figs 3, 4B, 5A). The conglomerates occur mostly as a single bed with a sharp basal contact and a thickness of 0.1 to 1 m. Conglomerates resting directly on the Buntsandstein at localities 8 and 12 (Fig. 4A) are well sorted and composed predominantly of spherical to discoid, rounded and well-rounded milky quartz pebbles, up to 5 cm in size, with a dispersed shell debris. At locality 12, pebbles show a preferential NE–SW orientation of their long axes (Fig. 5A) and weakly defined imbrication of bladed clasts. The conglomerate matrix is composed of moderately to well sorted, medium-grained lithic sand with a small admixture of glauconite. Conglomerates with the greatest thickness (up to 1 m), in the Płoszczyna Graben (locality 13), are predominantly clast-supported and consists of massive, lens-shaped beds (Fig. 5B) with a sandy matrix rich in glauconite. Where overlying discordantly the Permian and older metamorphic rocks in the Płoszczyna Graben, the conglomerates contain a small (up to 10%) admixture of tabular, bladed or rod-shaped cleaved metamorphic clasts of greenschists, metacherts and phyllites (locality 13; Fig. 5B). Although the pebbles in the conglomerate are rounded to well rounded, the matrix grains are predominantly angular and subangular. This continuous conglomerate bed is lacking in the northernmost sector of the WG (locality 8), where the poorly visible Triassic-Cretaceous unconformity is marked by a petrographic and subordinate colour difference between the Cretaceous and Triassic sandstones (Fig. 5C).

Conglomerates of the lowermost Wilków Member are usually massive (facies Gm/GSm; Table 1 and Fig. 5A) or normally graded (facies Gm_g/GSm_g), displaying tight packing of pebbles with dispersed coquina or shell lags visible predominantly as asymmetrical voids in the sandstone. Occasionally visible are bioturbation structures within and below the basal conglomerates, also in the underlying, weakly cemented Buntsandstein. Single, nearly vertical and slightly curved *Ophiomorpha* isp. up to 15 cm long and 0.5 cm in diameter, filled with medium-grained, massive, brown sand, occur also below the unconformity at localities 8 and 12 (Fig. 5C).

The conglomerates pass upwards into poorly to moderately sorted, greenish-grey to dark yellow, medium- to coarse-grained lithic and subordinately quartz arenites with an admixture of matrix-supported conglomerates (Fig. 4B). Grain framework is dominated by semi-rounded and semi-angular quartz grains, 0.3 to 0.6 mm in size, with a small contribution of angular and subangular lithic clasts,

up to 0.8 mm (Fig. 5D). Monocrystalline quartz grains are the most common, with an up to 10% contribution of polycrystalline grains. An admixture of white feldspars with automorphic or hypautomorphic outlines and less abundant lithic grains, up to 0.7 mm in size, occurs in grain framework in the upper part of the succession. The sandstones are well cemented, their matrix includes fine quartz grains and, at locality 13, an admixture of ovoid glauconite grains (Fig. 5D). Interbeds of fine-grained conglomerates composed of milky quartz clasts and crushed bivalve shells were also noted.

Sandstones of the Wilków Member are rather poorly stratified, with cross-stratification visible mostly in the lowermost part of the succession and poorly visible in the upper part. The sandstones locally show planar cross-stratification and subordinate trough cross-stratification (facies Sp and St, respectively; Table 1 and Figs 4B, 5E). Single cross-strata sets observed in small outcrops at localities 1–4 and 11 are up to 0.5 m thick, with foresets inclined towards the NW and W (Fig. 5E). Locally, at the base of the cross-stratified sandstones occur beds of massive conglomerates up to 10 cm thick (facies Gm/GSm). Cross-stratified sandstones are less common at localities 4 and 8–9, where only relics of trough and planar cross-stratification disturbed by bioturbation (facies St_r and Sp_r, respectively) were occasionally observed.

Stratified sandstones pass gradually upwards into massive (facies Sm/SGm) or normally graded sandstone beds (facies Sm_g) with scattered body fossils (*Lima* sp. and *Pecten* sp.) or continuous horizons of disarticulated shell debris (facies GSc/SGc; Table 1 and Fig. 5F). Individual beds are up to 0.5 m thick and bounded by sharp, undulating erosional bases, commonly overlain by continuous gravel lags composed of fragmented shell debris and quartz pebbles (facies GSc; Figs 4B, 5G). Sporadically observed are continuous horizons with convex-up accumulation of *Pecten*-like coquinas, represented by asymmetrical voids. Above the gravel and shell lags (facies GSm and GSc, respectively) occur lenticular packages of amalgamated pebbly sandstones, up to 10 cm thick, with faintly visible relics of hummocky and wave ripple cross-stratification (facies Su/Su_r and Srw/Srw_r, respectively; Fig. 5H) or sandstones with trough and planar cross-stratification (facies St and Sp, respectively). At localities 4–5, 10 and 13, sandstones are rich in bioturbation structures (facies Sb) including *Ophiomorpha* isp. and *Thalassinoides* isp., which form complex burrow systems on the lower surfaces of beds (Fig. 5I).

The uppermost part of the Wilków Member is poorly exposed in the WG area. Isolated outcrops of the topmost part of the sandstones were documented near the villages of Nielestno and Czernica (locality 9). They show ca. 4-m long sections of bioturbated (facies Sb) or massive sandstones (facies Sm) inclined steeply at up to 60° towards the SW. Numerous *Ophiomorpha* isp. and *Thalassinoides* isp. occur on the upper surfaces of the massive beds (Fig. 5J). Massive and bioturbated sandstones are gradually overlain by poorly sorted calcareous sandstones (observed almost only as blocks in scree cover), which pass upwards into calcareous mudstones and siltstones assigned to the Heterolithic Series (see below). The sedimentary contact of the non-calcareous sandstones of the Wilków Member with the overlying calcareous deposits remains unexposed.

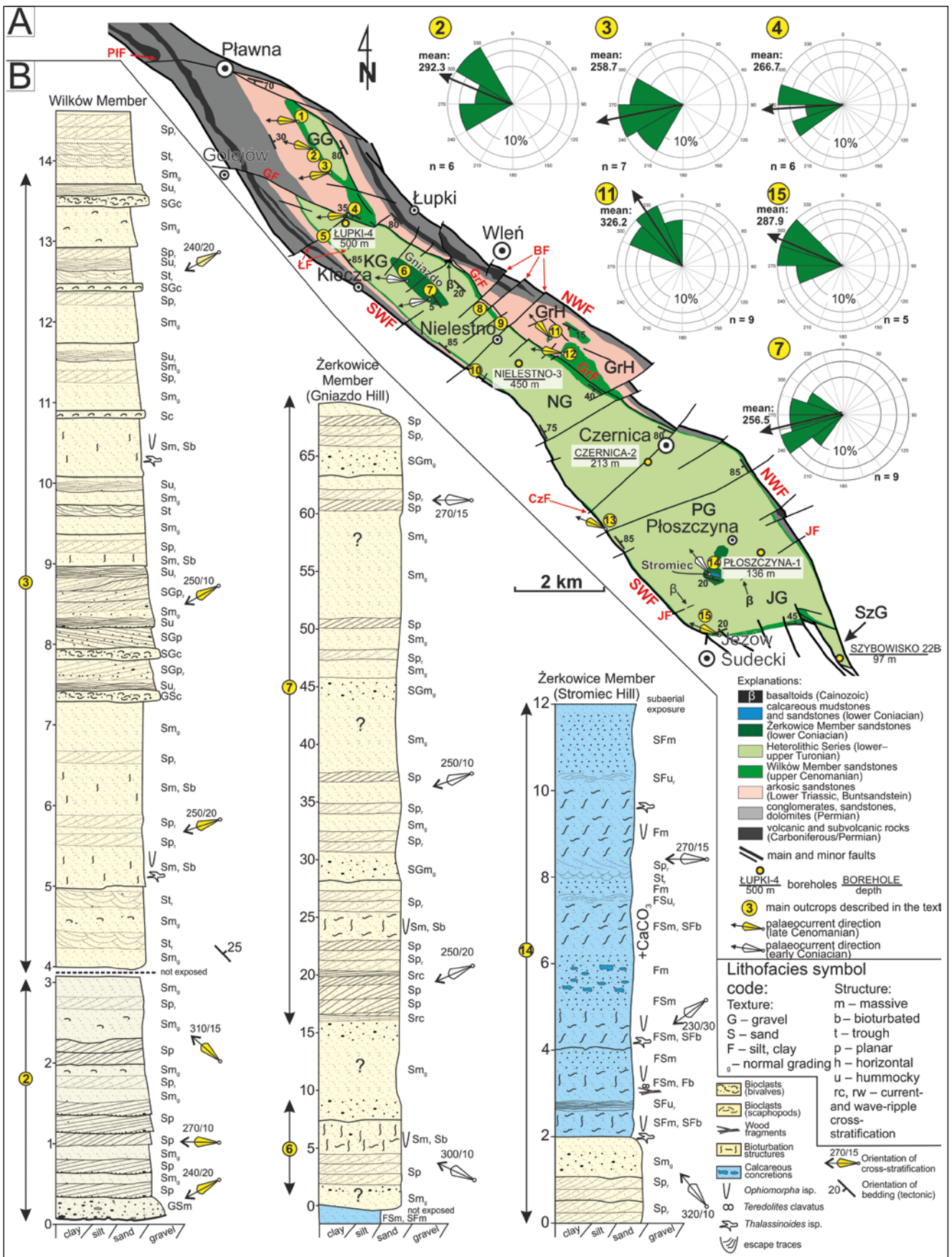


Fig. 4. Extent, tectonics and sedimentological features of the Upper Cretaceous in the Wleń Graben. **A.** Detailed geological map of the WG (made by the present author) with superimposed mean transport directions obtained from each locality. Note the location of individual boreholes. The inset rose diagrams (upper right corner) show the measured orientation of cross-stratification with its mean directions (black arrows) for selected localities. Letter symbols: BF – Bóbr Faults; CzF – Czernica Fault; GG – Golejów Graben; GF – Golejów

The Heterolithic Series (Turonian–Coniacian?). Fine-grained calcareous deposits referred to in this paper as the Heterolithic Series crop out mainly in the axial part of the WG and reach a thickness of nearly 300 m (borehole Nielestno-3; SPDPSH, 2019) in the deepest part of the graben. They are the main component of the Cretaceous succession preserved in the graben with regard to thickness and outcrop area (Fig. 4A), but are highly sensitive to weathering and sparsely exposed. Small outcrops of the Heterolithic Series, < 2m thick, occur in deeply incised stream valleys and road-cut sections in the southern and central segments of the WG (locality 14; Fig. 6A, B). Therefore, it is almost impossible to perform long-distance correlations and construct a reliable vertical succession of these deposits. Mapping survey is also insufficient in this case, due to strong tectonic deformation and a thick (up to 20 m) cover of Quaternary deposits.

The Heterolithic Series consist mainly of homogenous and soft, pale grey to dark grey mudstones with a small contribution of discontinuous siltstone and sandstone intercalations (Fig. 6B). Grey mudstones are predominantly composed of detrital quartz grains, 0.02 to 0.1 mm in diameter, and subordinate feldspar and lithic grains cemented with a carbonate to siliceous matrix that amounts in some cases up to 75 vol.% (Fig. 6C). A small admixture (up to 5%) of glauconite grains up to 0.25 mm in size is also present (Fig. 6C, D). Intercalations of poorly sorted, yellowish to grey calcareous sandstones occur only locally, particularly in the lowermost and uppermost parts of the Heterolithic Series. Moreover, the mudstones in the middle part of the succession contain numerous pillow-shaped calcareous concretions, up to 25 cm in length (Fig. 6B), composed of recrystallized carbonate with a considerable amount (up to 10%) of glauconite.

The Heterolithic Series show mainly flat-lying, strongly fractured beds of fine-grained sandstone and mudstone/siltstone alternations that seem to be internally massive, lacking primary sedimentary structures (facies SFm and Fm, respectively; Table 1 and Fig. 6A, B). Locally observed are sparse relics of horizontal or subhorizontal, parallel, undulating lamination or subtle mottling associated with grain-size changes. Mudstones and fine-grained sandstones are variably bioturbated, with predominantly *Ophiomorpha* isp. and numerous undetermined trace fossils (facies Sb, Fb). Body fossils are relatively rare and include disarticulated shells of inoceramids pointing to Turonian and early Coniacian age (Gorczyca-Skała, 1977). Other macro- and microscopic bioclasts found in the mudstones include isolated, undetermined crushed fragments of white-coloured shell debris. The poor exposure of calcareous heterolithic deposits precludes more detailed observations.

The Upper Jointed Sandstone (Żerkowice Member, lower Coniacian). The Żerkowice Member sandstones were not drilled (Fig. 4A) and are exposed in only two areas

(localities 6/7 and 14) which are the Gniazdo and Sromiec hills in the axial part of the WG. The preserved remnants of the Żerkowice Member sandstones attain a thickness of ca. 80 m and surface area of 0.2 km² in the Stromiec Hill, and 65 m and ca. 0.5 km² in the Gniazdo Hill. The lowermost part of the sandstones is exposed in localities 6/7 (Fig. 7A), whereas the uppermost part crops out only at the top of the Stromiec Hill (locality 14; Fig. 7B). Well exposed is only the uppermost, calcareous part of the succession, up to 12 m thick, as a large part of the sandstones is covered by slope talus and inaccessible to direct observations.

This lower Coniacian in the WG consists of poorly to well sorted, weakly cemented, pale-yellow to light grey, medium- to coarse-grained arkosic and quartzose arenites, with a small admixture of granules (estimated at up to 5%). The framework is composed chiefly of semi-angular to subrounded quartz grains, up to 1.5 mm in size, whose content reaches up to 90%. Grains of 0.4 to 0.7 mm size dominate. The upper part of the succession in Stromiec Hill contains also white feldspar grains (up to 10%), most of them completely altered into kaolinite. The kaolinite content of sandstones on the Stromiec Hill is higher than on the Gniazdo Hill, which makes the non-calcareous sandstones weaker lithified. A clay-siliceous matrix is present in the sandstones.

In the upper part of the Gniazdo Hill, the pure and well-sorted quartz arenites are composed almost exclusively of well rounded, spherical quartz grains up to 1 mm in size. In the uppermost part of the Żerkowice Member at the top of Stromiec Hill, poorly sorted calcareous sandstones overlie the non-calcareous sandy deposits, with a framework of semi-angular to subrounded quartz grains, mainly 0.2 to 0.6 mm in size, and an admixture of feldspar and lithic grains and crushed bioclasts (10%). The cementing matrix is micrite, coloured by iron oxides. These are the youngest preserved remnants of Cretaceous deposits in the WG.

The lowermost part of the Żerkowice Member exposed in abandoned quarries on the Gniazdo Hill consists mainly of massive sandstones (facies Sm; Figs 4B, 7A) with a distinct admixture of thoroughly bioturbated sandstones (facies Sb) as well as relics of wedge-shaped sets of planar cross-strata (facies Sp). They pass upwards into massive, locally intensely bioturbated sandstones (facies Sb) containing burrow system *Thalassinoides* isp. and single *Ophiomorpha* isp. shafts reaching down from the bed tops to nearly 0.2 m. Numerous small horizontal burrows and unidentified trace fossils are also present (Fig. 7C). The bioturbated sandstones pass upwards into cross-stratified sandstones, exposed in the middle part of the poorly accessible outcrop section at Białe Ściany (locality 7; cf. Fig. 4B). The lower part of the outcrop walls consists of vertically stacked, unidirectional sets of tangential planar cross-strata (facies Sp; Table 1 and Figs 4B, 7D) with set thicknesses of up to 0.5 m and dips towards the NW and WNW. They are

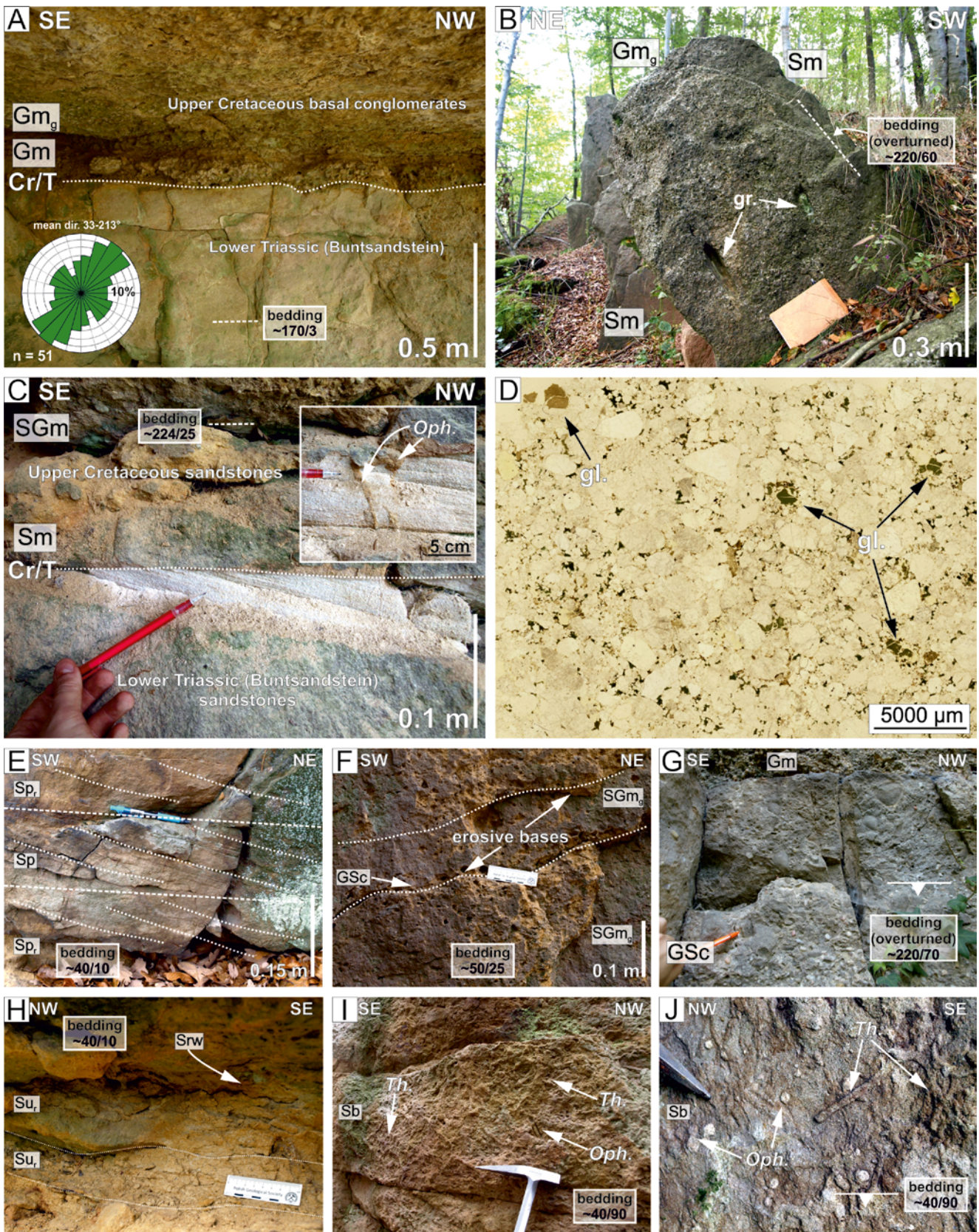


Fig. 5. Sedimentary features of the Wilków Member sandstones in the Wleń Graben. **A.** The “basal conglomerate”: sharp-based bed of massive (facies Gm) and normally-graded (facies Gm_g) clast-supported conglomerates discordantly overlying Buntsandstein; locality 12. Clast *a*-axes exhibit prevalent NE–SW orientation (see inset rose diagram). **B.** Bed of clast-supported, normally-graded conglomerates (facies Gm_g) in the lowermost part of the Wilków Member sandstones (overturned) at locality 13. Note the metamorphic greenschist clasts in conglomerate (gr.; white arrows). **C.** Sharp-based bed of Wilków Member massive sandstones (facies Sm) discordantly overlying Buntsandstein at locality 8. Note the lack of “basal conglomerate” and the Triassic-Cretaceous unconformity (Cr-T) marked by petrographic and colour change in sandstones. The inset close-up shows nearly vertical *Ophiomorpha* isp. (*Oph.*) reaching down below

separated by planar or slightly concave upwards surfaces gently inclined at 5° in the same direction. The individual sets of cross-strata contain erosional reactivation surfaces. The planar cross-stratified sandstones pass upwards into an alternation of massive and planar cross-stratified quartzose sandstones in the topmost part of the Gniazdo Hill (localities 6/7; cf. Fig. 4B), which are probably a time-equivalent of the non-calcareous quartz arenites exposed in the upper part of the Stromiec Hill (locality 14), directly below the calcareous sandstones and mudstones.

The non-calcareous quartz sandstones, exposed in small isolated outcrops (size up to 2 m) at the summit of Stromiec Hill are sharply overlain by a unit of calcareous heterolithic deposits 12 m thick (Fig. 4B). Non-calcareous arenites show relics of planar cross-stratification (facies Sp_r), with cross-sets up to 0.2 m thick and built towards the WNW and NW. Body fossils and bioturbation structures are extremely rare, observed only in detached rock blocks. Two poorly preserved imprints of unassignable bivalve shells (inoceramids?; Fig. 7E) as well as driftwood fragments with casts

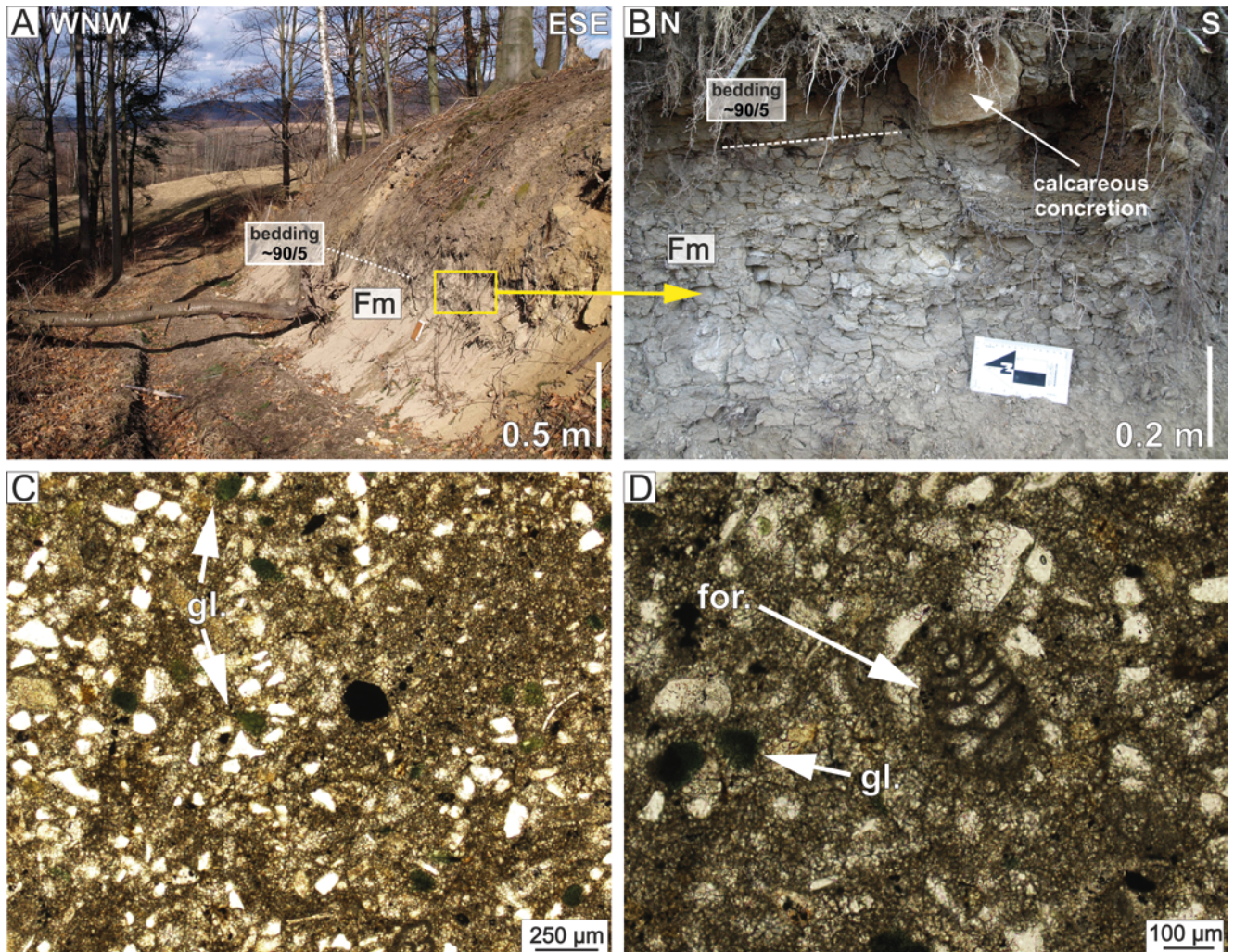


Fig. 6. Sedimentary features of the Heterolithic Series in the Wleń Graben. **A.** Small outcrop section of massive calcareous mudstones (facies Fm) at locality 14. **B.** Strongly fractured massive calcareous mudstones (facies Fm) with pillow-shaped calcareous concretions in the upper part of outcrop at locality 14. **C, D.** Microscopic views of calcareous mudstones from locality 14, composed mainly of dispersed detrital quartz grains cemented by carbonate. Note the dispersed and partly crushed bioclasts of single foraminifers (for.) and a small admixture of green authigenic glauconite (gl.).

the Triassic-Cretaceous unconformity into the weakly cemented Buntsandstein. **D.** Microscopic view of coarse-grained sandstones (locality 13) composed mainly of subangular quartz grains with admixture of green glauconite (gl.), cemented with siliceous matrix. **E.** Planar cross-stratified sandstones (facies Sp and Sp_r) at locality 11. **F.** Normally-graded gravelly sandstones (facies SGM_g) bounded by sharp, undulating erosional bases overlain by continuous gravel and shell lags (facies GSc), locality 3. **G.** Continuous lag composed of quartz pebbles and shell debris of *Pecten* sp. (facies GSc) on a vertically-oriented, upper surface of sandstone bed at locality 13. **H.** Lenticular packages of sandstones with relic hummocky stratification (facies Su_r) and wave ripple cross-lamination (facies Srw) at locality 1. **I.** Burrow systems *Ophiomorpha* isp. (*Oph.*) and *Thalassinoides* isp. (*Th.*) on a vertically oriented lower surface of sandstone bed (facies Sb) at locality 10. **J.** *Ophiomorpha* isp. (*Oph.*) and *Thalassinoides* isp. (*Th.*) on the upper surface of bioturbated sandstone bed (facies Sb) at locality 9.

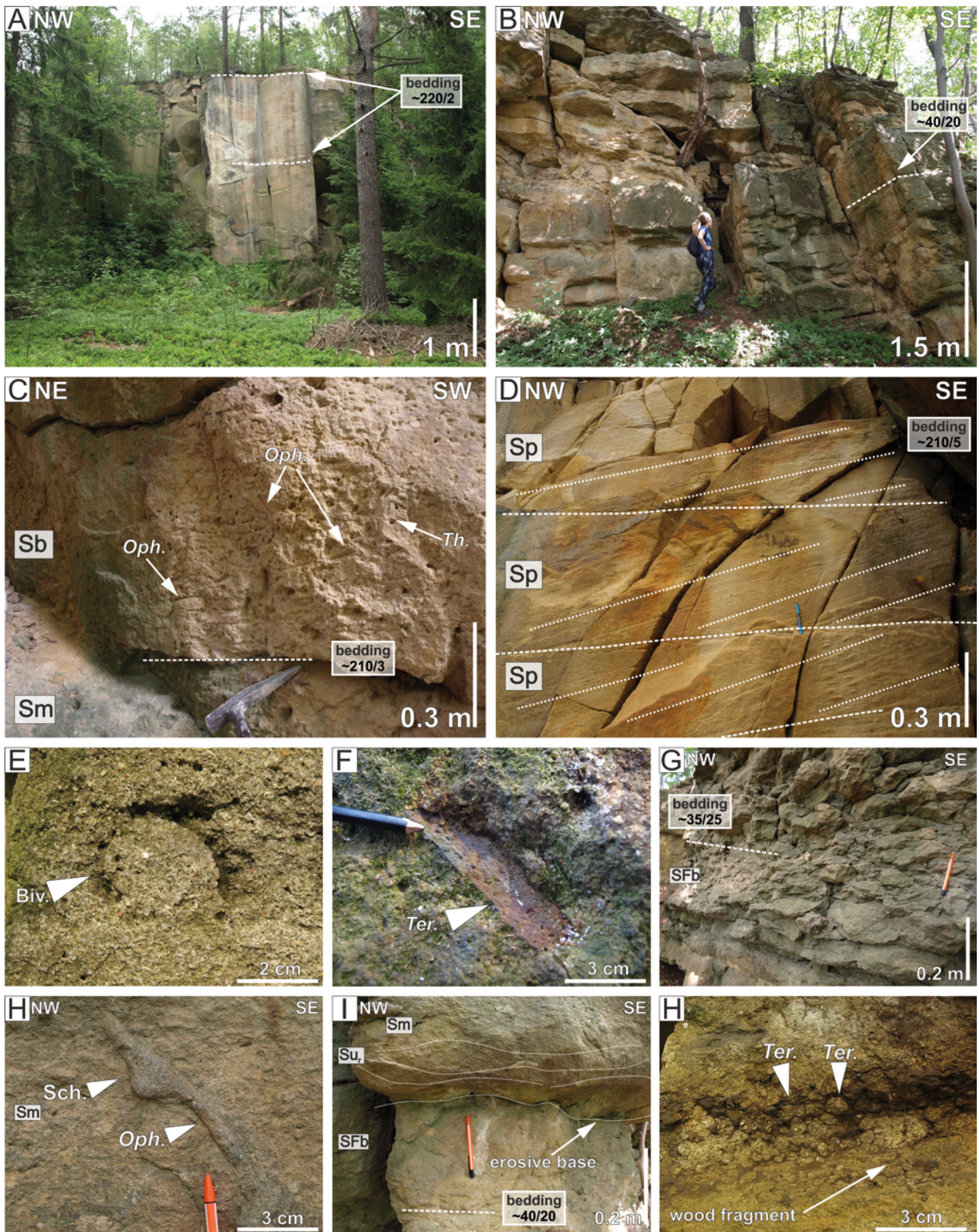


Fig. 7. Sedimentary features of the Żerkowice Member sandstones in the Wleń Graben. **A.** Thick-bedded massive sandstones in the lowermost part of the Żerkowice Member in an abandoned quarry at locality 6. **B.** Weakly lithified and weathered calcareous sandstones of uppermost Żerkowice Member at locality 14 (Stromiec Hill). **C.** Intensely bioturbated sandstones with systems of *Thallasinoides* isp. (*Th.*) and *Ophiomorpha* isp. (*Oph.*) at locality 6. **D.** Vertically stacked, unidirectional sets of planar cross-strata (facies Sp) in the lowermost part of Białe Ściany at locality 7. **E.** Imprint of unassignable bivalve shell (*Biv.*; inoceramid?) in loose block of non-calcareous sandstone on the slope of Stromiec Hill (locality 14). **F.** Fragment of driftwood with poorly visible *Teredolites clavatus* (*Ter.*) in loose block of non-calcareous sandstone on the slope of Stromiec Hill (locality 14). **G.** Intensely bioturbated muddy sandstones (facies SFb) at locality 14

of bivalve wood borings (*Teredolites clavatus* Leymerie; Fig. 7F) were also found in loose rock blocks. A specimen of a Coniacian bivalve *Inoceramus subquadratus arrondatus* Heine was reported from the Żerkowice Member in WG by Gorczyca-Skała (1977).

The base of the calcareous sandstones above the non-calcareous strata is sharp and probably erosional. Fine-grained sandstones overlying this surface are predominantly massive (facies SFm) and pass into intensely bioturbated muddy sandstones (facies SFb) or sand-rich mudstones (facies FSb; Figs 4B, 7G), locally intercalated with massive, thin silty and clayey horizons (facies Fm). Individual sandstone beds attain thicknesses of up to 1 m, whilst the silty and clayey intercalations are up to 0.05 m thick. Within mudstones occur numerous completely burrowed horizons, containing *Thalassinoides* isp. and *Ophiomorpha* isp. with abundant swollen chambers (Fig. 7H; e.g., Chrzastek and Wypych, 2018). Above the bioturbated horizons occur lens-shaped packages of fine- to medium-grained calcareous sandstones with floating granules of up to 0.4 cm in size. They show faint relics of hummocky cross-stratification (facies Su₁) with undulating, sharp bases overlain by lens-shaped packages of gently inclined strata (Fig. 7I). Relics of small-scale trough cross-stratification were also observed (facies St₁; Fig. 4B). The stratified horizons pass upwards into completely bioturbated, fine-grained sandstones, locally rich in calcareous concretions. They show slightly curved vertical and horizontal *Ophiomorpha* isp. and *Thalassinoides* isp., circular or strongly flattened in cross-sections. Body fossils have not been found, although possible sand-filled remnants of bivalve shells (inoceramids?) in life position were observed in vertical cross-sections. Rarely, within the calcareous sandstones occur scattered, up to 10 cm long, fragments of dark brown driftwood with well-preserved, aggregated casts of bivalve wood borings (*Teredolites clavatus*; Fig. 7J). The topmost part of the calcareous sandstones at locality 14 corresponds to the present-day subaerial erosional exposure.

Upper Cretaceous in the Krzeszów Brachysyncline

Spatial extent, tectonics and stratigraphy

The Upper Cretaceous in the KB, assigned to the Krzeszów Formation, occurs as a relatively continuous cover (Fig. 8). The strata represent stratigraphic intervals ranging from the upper Cenomanian to the lower(?) Coniacian and cropping out both along the axis and the elevated limbs of the KB (Fig. 8). The youngest strata – assigned to the Gorzeszów Member, Upper Heterolithic Series and the Krzeszów Member (Figs 3 and 8) – occupy the axial zone of brachyfold near the villages of Gorzeszów and Krzeszów and are inclined gently at up to 15° towards the NW–SE axis of the KB (Fig. 8). The elevated limbs of the KB are generally composed of the upper Cenomanian to lower Turonian strata of the Zawory Member and the Lower

Heterolithic Series, forming monoclinical structures dipping at 10–30° towards the KB axis.

According to Jerzykiewicz (1969, 1971), the KB is bounded from the north and south by marginal flexures built of tilted (up to 25°) Cretaceous rocks, with the flexural bends corresponding to the slopes of the Drogosz and Góra Świętej Anny hills in the southernmost and northernmost parts of the KB, respectively. To the south-east, through the WNW–ESE trending Łączna Elevation, previously called the Łączna Anticline or Łączna Brachyanticline (Jerzykiewicz, 1969, 1971; Don *et al.*, 1981a, b), the KB borders on the NW–SE trending Police Brachysyncline, located mainly in the Czech Republic (Fig. 8). The Cretaceous and Triassic strata within this structure are horizontal or dip gently towards the north at up to 15° within the Southern Marginal Flexure of the KB and to the south towards the Police Brachysyncline. The tectonic setting of this area was re-assessed by Kowalski (2017), who interpreted the Łączna Elevation area as a NW–SE trending transtensional structural high (tectonic horst) bounded by a system of NW–SE trending strike-slip and normal faults, separating the KB and Police Brachysyncline.

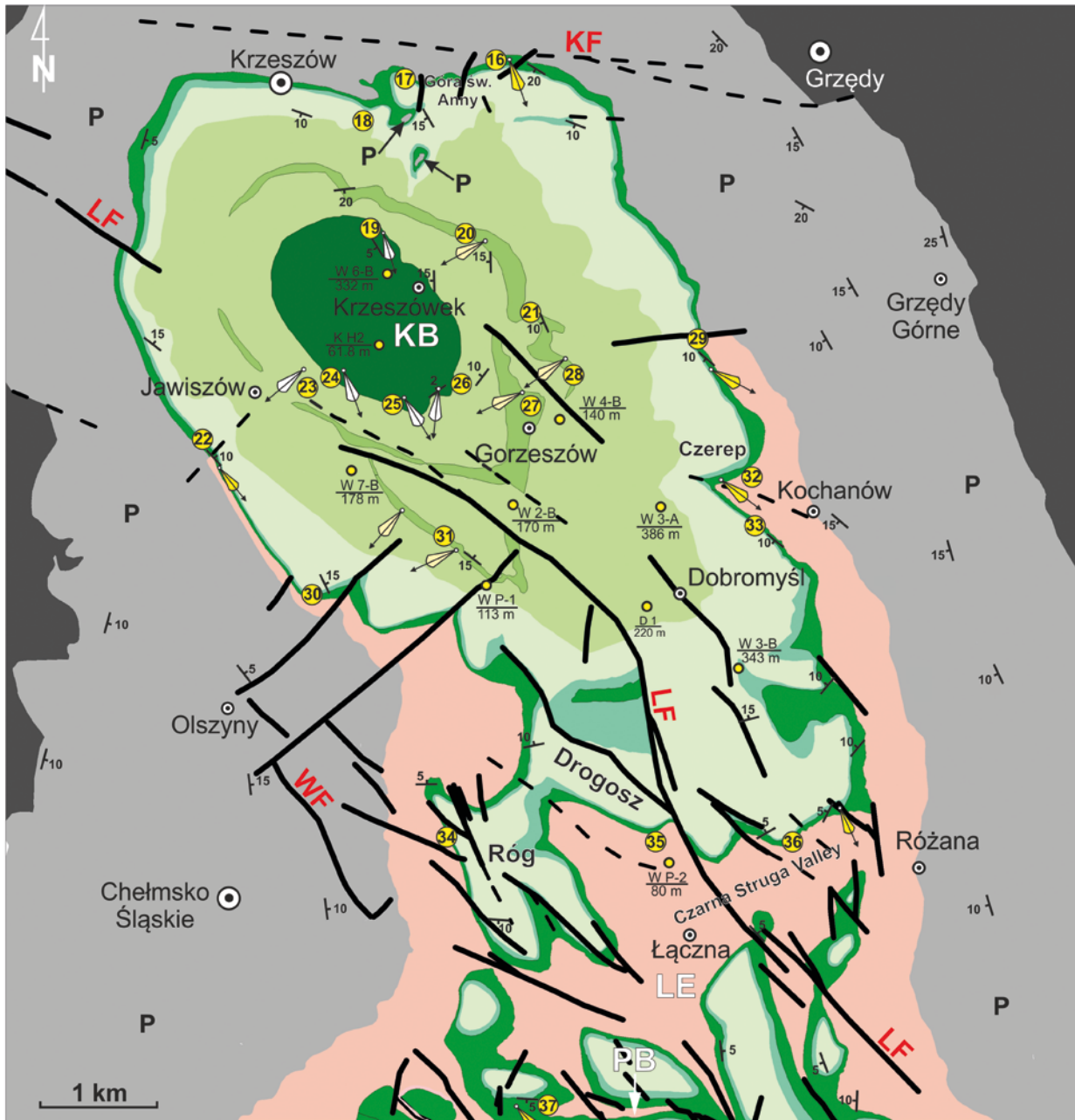
The most significant fault zone dissecting both the Łączna Elevation and Krzeszów Brachysyncline is the Lipienica–Łączna Fault (Don *et al.*, 1981b), with a throw reaching ca. 20 m in the southern part of the KB. The second important dislocation, called the Wójtowa Fault (Fig. 8; Don *et al.*, 1981b), cuts Permian deposits in the western part of the Łączna Elevation. The northern part of the KB is dissected by the WNW–ESE trending Krzeszów Fault and several minor dislocations trending mainly NE–SW.

Lithology, petrography and sedimentary facies

The Lower Jointed Sandstone (Zawory Member, upper Cenomanian). The lowermost part of the Cretaceous succession in the KB area is represented by a single, continuous sandstone horizon (Lower Jointed Sandstone) assigned to the upper Cenomanian (Jerzykiewicz, 1971; Don *et al.*, 1981a, b). This sandstone unit is referred to herein as the Zawory Member (Fig. 3) which corresponds to the Peruc-Koryčany Formation in the Czech part of the Intra-Sudetic Synclinorium area (Dvořák, 1968; Čech *et al.*, 1980) and to the Wilków Member in the North Sudetic Synclinorium area (Milewicz, 1985). The sandstones have a relatively uniform thickness, reaching 10 m in the southern (localities 34–36) and eastern parts (localities 29 and 33) of the KB area. In borehole Dobromyśl-1 (D1 in Fig. 8; Wojtkowiak *et al.*, 2009), in the central sector of the KB, the non-calcareous sandstones of the Zawory Member reach a thickness of 5.5 m and pass gradually upwards into dark-grey calcareous sandstones of the Lower Heterolithic Series. A similar thickness of the Zawory Member, ca. 6.5 m, is found in the northernmost part of the KB (locality 16).

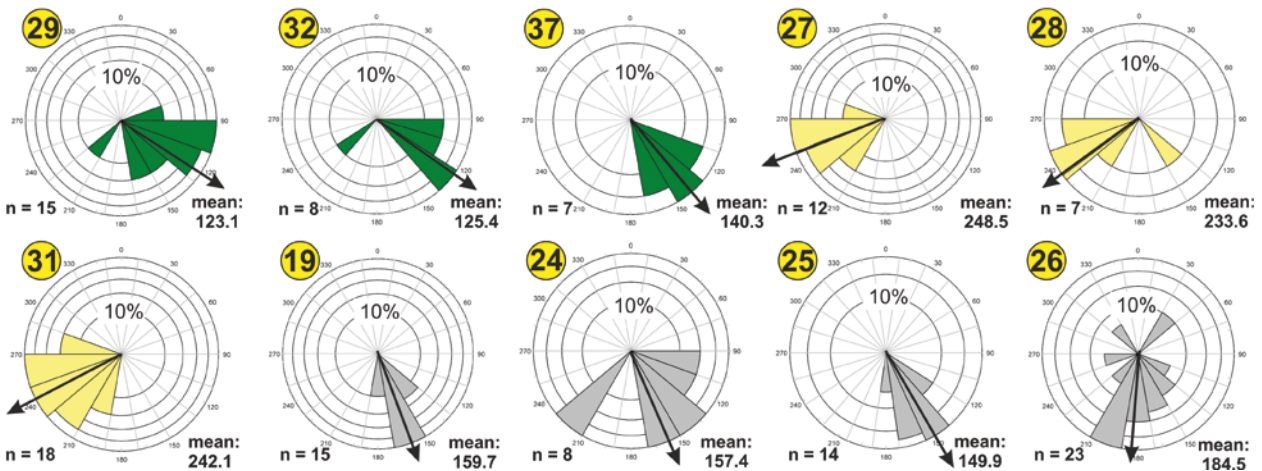
As in the WG area, the lowermost part of the Lower Jointed Sandstone in the KB consists of a relatively well

(Stromiec Hill). **H.** *Ophiomorpha* isp. (*Oph.*) with swollen chamber (Sch.) in a massive fine-grained sandstones (facies Sm) at locality 14. **I.** Lens-shaped packages of calcareous sandstones with relic hummocky stratification (facies Su₁) underlain by sharp erosional base, locality 14. **J.** Driftwood fragment with aggregated bivalve wood borings (*Ter.*; *Teredolites clavatus*) at locality 14.



Explanations:

- Krzeszów Member sandstones (upper Turonian-lower Cenomanian)
- calcareous sandstones and mudstones (LHS; upper Cenomanian)
- calcareous mudstones and sandstones (LHS + UHS; lower-upper Turonian)
- Zawory Member sandstones (upper Cenomanian)
- Gorzeszów Member sandstones (middle Turonian)
- arkosic sandstones (Lower Triassic, Buntsandstein)
- siliceous mudstones and sandstones (LHS, upper Cenomanian)
- conglomerates, sandstones (Lower Permian, Rotliegend)
- volcanic and subvolcanic rocks (Carboniferous/Permian)
- paleocurrent direction (late Cenomanian)
- paleocurrent direction (middle Turonian)
- paleocurrent direction (late Turonian/early Coniacian)
- main and minor faults
- boreholes $\frac{\text{BOREHOLE}}{\text{depth}}$
- 20 main outcrops described in the text



sorted, yellowish-green to grey, clast-supported “basal” conglomerate (facies Gm/GSm and Gm_g/GSm_g; Table 1 and Figs 3, 9) that has a sharp, undulating base and a thickness of 0.15 to 0.5 m (Fig. 10A). The conglomerate consists of spherical to discoid, rounded and well-rounded milky quartz pebbles. In the northernmost part of the KB (locality 16), conglomerate clast framework contains scattered disarticulated shell debris of *Lima* sp. as well as an admixture of dark grey or black metacherts (lydites; up to 10% of framework) and creamy-pinkish rhyolites (up to 15% of framework), with clasts up to 12 cm in size. Bladed and tabular clasts display a preferred NNW–SSE orientation of their *a*-axes (Fig. 10A) and a weak imbrication. At locality 22 (abandoned quarry in Jawiszów), the clast-supported basal conglomerate occurs as two massive beds, up to 15 cm thick, composed of well-rounded quartz pebbles up to 3 cm in size and a matrix of moderately to well sorted, medium-grained lithic sand with a small admixture of glauconite.

The basal conglomerate is overlain by medium- to coarse-grained sandstones that locally display high mineralogical and textural maturity. Sandstones are pale- to dark-grey, texturally mature to super-mature quartz arenites, containing of up to 98% rounded and well-rounded, spherical and discoidal quartz grains with small admixture of strongly kaolinized subrounded feldspar grains in the southern part of the KB (locality 34; Fig. 10B). Locally, the normal-graded sandstone beds have basal parts (up to 0.1 m in thick) rich in granules, with quartz grains up to 0.5 cm in size. These quartzose arenites, with a thickness of up to 2 m, are exposed only at localities 22, 29 and 32. They pass upwards into moderately to poorly sorted, yellowish-grey to dark greenish-yellow sandstones classified as medium- and fine-grained, lithic and sublithic arenites. Their framework mass is composed chiefly (up to 80%) of angular and subrounded quartz grains, 0.35 to 0.6 mm in size, with an admixture of strongly altered plagioclase or microcline, light-coloured mica flakes, as well as lithic grains (gneisses, metacherts and Permian volcanic rocks). Some of the largest, subrounded quartz grains, up to 2 mm in size, display hexagonal outlines (Fig. 10B). The brownish cement (up to 10%) is mostly siliceous or argillaceous, with an admixture of ferric oxides and aggregates of brown to green glauconite (Fig. 10B).

The Zawory Member sandstones at localities 29, 32, 34 and 35 show planar angular cross-stratification (facies Sp; Figs 9, 10C, D). The cross-strata sets have near-horizontal bases, attain a thickness of up to 0.3 m and are inclined mainly to the SE. Their basal parts locally show blankets of granule gravel up to 5 cm thick (facies GSm_g; Fig. 10D). At locality 29 (Żłób Pass), the planar cross-stratified sandstones pass upwards into trough cross-stratified sandstones (facies St; Fig. 9). They are generally weakly bioturbated, although above the Triassic-Cretaceous unconformity locally occur single trace fossils including *Ophiomorpha* isp. and

Thalassinoides isp. (Figs 9, 10E, F). Cross-stratified sandstones are overlain by normally graded (facies Sm_g) or massive (facies Sm) yellowish sandstones with relic cross-stratification (Fig. 9). These occur in several abandoned quarries in the whole KB area (localities 22, 33–37) and form beds up to 0.8 m thick with sharp erosional boundaries (Figs 9, 10G). In their lower parts occurs shell hash with an admixture of well-rounded quartz granules up to 0.5 cm in size. Solitary coquina beds, made predominantly of *Lima* sp. and *Pecten asper* G. B. Sowerby II in Reeve shells in concave-upwards positions, form laterally extended lags (facies GSc; Table 1) that locally occur as lens-shaped clusters. At locality 37 (Libna quarry), four such continuous horizons were noted (Fig. 9). Moreover, the middle part of profile at localities 33 and 37 shows shell lags containing crushed and chaotically arranged scaphopod moulds representing *Dentalium sexcarinatum* Münster in Goldfuss (Fig. 10H) that are overlain by sandstones with relics of low-angle, possibly hummocky, stratification arranged into sets up to 10 cm thick (facies Su_r; Table 1 and Fig. 9). They pass upwards into sandstones beds that are massive, slightly normal-graded (facies Sm_g) and bioturbated (facies Sb), with relic wedge-shaped planar cross-strata sets (facies Sp) disturbed by single vertical *Ophiomorpha* isp. Locally found are accumulations of rafted wood fragments, up to 0.6 m in length, with casts of bivalve wood boring *Teredolites clavatus* (Fig. 10I, J). The lithic arenites of the Zawory Member pass gradually upwards into calcareous sandstones of the Lower Heterolithic Series (see below).

The Lower Heterolithic Series (upper Cenomanian–lower Turonian). The Lower Heterolithic Series occurs between the sandstones of the Zawory and Gorzeszów members and is dominated by fine-grained, carbonate and siliciclastic deposits. From the base upwards, the Lower Heterolithic Series comprises calcareous sandstones and mudstones followed by siliceous and glauconitic mudstones (gaizes) that pass upwards into calcareous mudstones (Fig. 3). These deposits are assigned to the upper Cenomanian (calcareous sandstones to siliceous mudstones; Jerzykiewicz, 1971; Tisseyre, 1972) and the lower Turonian (topmost calcareous mudstones; Jerzykiewicz, 1971), and together attain a thickness of up to 150 m in the central part of the KB. Due to their high resistance to weathering, the siliceous mudstones form the highest elevations of homoclinal quaternary ridges and used to be mined in several quarries for the road building purposes.

The lowermost, poorly exposed part of the Lower Heterolithic Series, consists typically of medium- to coarse-grained, dark-grey, weakly cemented calcareous sandstones, locally with thin (up to 5 cm) mudstone intercalations. In borehole D1 (Fig. 8; Wojtkowiak *et al.*, 2009), the vertical transition from the Zawory Member non-calcareous lithic

Fig. 8. Detailed geological map of the Krzeszów Brachysyncline (made by the present author) showing the extent of Upper Cretaceous and the location of outcrops and relevant boreholes. The measured mean transport directions for each locality are superimposed on the map. The rose diagrams in the lower part of the figure show the orientation of cross-stratification with their mean directions (black arrows) for selected localities. Letter symbols: KB – Krzeszów Brachysyncline; KF – Krzeszów Fault; LE – Łączna Elevation; LF – Lipienica-Łączna Fault; LHS – Lower Heterolithic Series; PB – Police Brachysyncline; UHS – Upper Heterolithic Series; WF – Wójtowa Fault.

sandstones to the Lower Heterolithic Series is relatively abrupt, yet with no obvious evidence of erosion. Historical photographs from the quarries in Łączna show the transition as marked by a change in the degree of weathering and fracturing of the sandstones, with the non-calcareous sandstones apparently massive and forming large angular blocks, and the calcareous ones strongly weathered and fractured (Fig. 11A). The calcareous sandstones are poorly sorted and composed chiefly of angular to subrounded detrital quartz grains, 0.2 to 1 mm in size (up to 70% of grain framework), white and partly kaolinized feldspar grains up to 0.5 mm in size, a small admixture of glauconite grains, scattered mica flakes and lithic grains (ca. 10% of framework). Their cement is micrite or sparite, with a content of up to 35%. In the upper part of the Libna Quarry (locality 37), up to 15 cm thick interbeds of poorly sorted, yellowish-grey, non-calcareous lithic sandstones occur within the calcareous sandstones (Fig. 11B). Above the sandstones occur calcareous mudstones, up to 10 m thick, passing upwards into non-calcareous, well-cemented, siliceous mudstones or fine-grained sandstones with spongiolites (gaizes; Fig. 11C). They are composed of fine and very fine detrital quartz grains, up to 0.1 mm in size, chlorite and mica flakes, as well as scattered chalcedonic sponge spicules. Cement is recrystallized silica, with a content exceeding 50% (Fig. 11D). In the lowermost part of the siliceous mudstones, ca. 5 m above their boundary with calcareous mudstones, occurs a glauconite-bearing unit (up to 0.5 m thick) referred to earlier as the glauconitic horizon (Berg and Dathe, 1905/1906, 1940). It consists of mudstones and fine-grained sandstones with dispersed nodules and aggregates of glauconite (glauconite peloids according to Ziółkowska, 1990), locally forming up to 50% of the grain framework (Fig. 11E, F). Dispersed organic matter occurs within black clayey intercalations at locality 30 (Fig. 11C, G). Numerous irregular discontinuous horizons of chert nodules, pale grey through creamy-yellow to brown and up to 0.3 m thick, were observed in the upper part of the siliceous mudstones (Fig. 11H, I) and referred to earlier as spongiolites (Jerzykiewicz, 1971). Their upward transition into weakly cemented calcareous mudstones is exposed in only one small outcrop between the villages of Gorzeszów and Olszyny (locality 31).

Similarly to the Turonian Heterolithic Series in the WG area, the Lower Heterolithic Series is represented by strongly fractured, fine- to coarse-grained sandstones that generally lack recognizable primary sedimentary structures. The individual beds in the lowermost part of calcareous sandstones are up to 15 cm thick and predominantly massive (facies Sm/SFm; Table 1 and Figs 9, 11B). Locally preserved in calcareous sandstones are sparse relics of horizontal or subhorizontal undulating stratification and normal grading from medium- to fine-grained sand (facies Sm_g), with faint flat lamination observed also in glauconitic mudstones (facies Fh/SFh). All lithologies within the Lower Heterolithic Series are locally heavily bioturbated (facies

Sb/SFb, Fb), with single beds of calcareous sandstones almost completely burrowed, whereas bioturbation structures in the siliceous mudstones occur only as single isolated burrows of *Ophiomorpha* isp. (Figs 9, 11B). Interestingly, glauconite is practically absent within the burrows. The siliceous mudstones ca. 3 m above the glauconitic horizon are rich in body fossils including moulds of inoceramid shells and accumulations of shell debris, including *Inoceramus pictus* Sowerby characteristic of the upper Cenomanian, as well as bivalves *Janira*, *Camptonectes*, *Pinna*, *Mytilus* and others (cf. Jerzykiewicz, 1971; Kowalski, 2015).

The Middle Jointed Sandstone (Gorzeszów Member, middle Turonian). The Middle Jointed Sandstone, assigned herein to the Gorzeszów Member (Fig. 3), occurs as a clinoformal sandy lithosome exposed near Gorzeszów, in the central part of the KB (Fig. 8). The lithosome has a maximum thickness of ca. 80 m and thins out towards the W and NW between the Lower Heterolithic Series and Upper Heterolithic Series. The best outcrops of the Gorzeszów Member are in the western limb of the KB, forming a prominent questa escarpment known as the Gorzeszowskie Skały (Gorzeszowskie Rocks) and Głazy Krasnoludków (Dwarfs Boulders; locality 31). The outcrops are numerous picturesque clusters of tors and isolated rock towers and hoodoos. The Gorzeszów Member is also exposed in the opposing, eastern limb of the KB, where it forms series of natural tors and indistinct questa ridges (localities 20–21, 28), and as an isolated tor called Diabelska Maczuga (Devil's Club) in the village of Gorzeszów (locality 27). The Gorzeszów Member has been briefly described in geological reports since the early 20th century (Flegel, 1904).

The main horizon of the Gorzeszów Member is composed of moderately to well sorted and moderately cemented, pale yellow to yellowish-grey, medium- to coarse-grained sandstones classified as subarkosic arenites, with a small contribution of granule-rich sandstones or sandy conglomerates in the lower part of this horizon. The grain framework consists mainly (up to 75%) of subangular to subrounded quartz grains, typically up to 2 mm in size, with a small admixture of completely kaolinized, angular and subangular grains of white feldspars (without feldspar cores; up to 8% of the framework) and lithic grains. Grains with diameters of 0.25 to 0.7 mm dominate, cemented with a clay-siliceous matrix. The lowermost part of the Gorzeszów Member contains texturally mature, well sorted, white to pale-grey, almost monomineral quartzose sandstones.

The lowest part of the Gorzeszów Member is well exposed in small tors at the eastern limb of the KB (localities 20–21, 28) and in the Diabelska Maczuga tor (locality 27; Fig. 12A). The bases of these tors are exposed ca. 3 m above the boundary with the underlying mudstone of the Lower Heterolithic Series. Quartzose and subarkosic sandstones show poorly visible planar cross-stratification and subordinate trough cross-stratification (facies Sp/Sp_r and St/St_r

Fig. 9. Synthetic sedimentological logs from selected Upper Cretaceous outcrops in the Krzeszów Brachysyncline (localities 16, 19, 23–25, 27, 29, 31 and 37 in Fig. 8). Main component sedimentary facies and other observed features observed are indicated in the logs, with facies letter code as in Table 1.

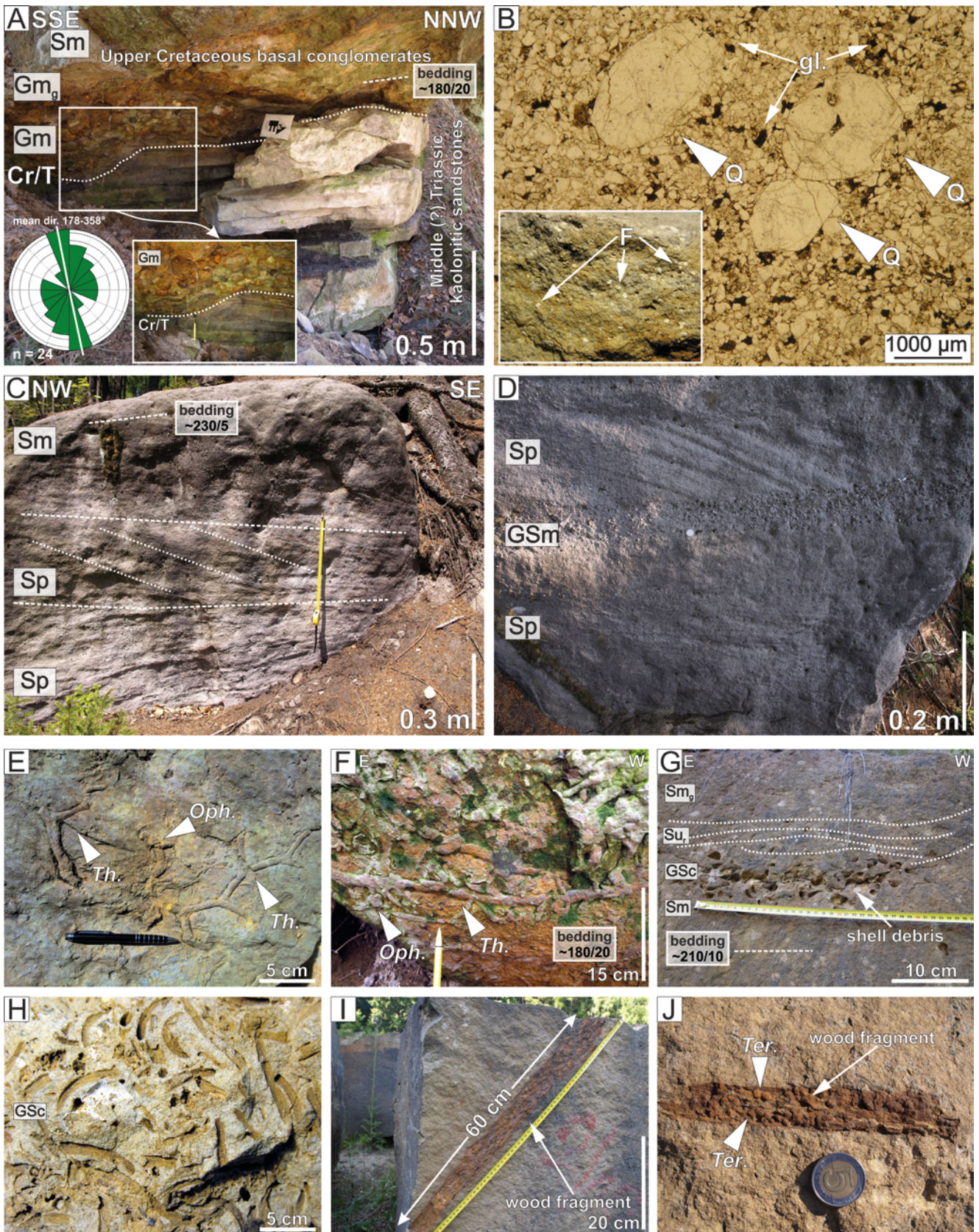


Fig. 10. Sedimentary features of the Zawory Member sandstones in the Krzeszów Brachysyncline. **A.** Sharp-based bed of massive, clast-supported conglomerates (facies Gm/Gm_g) overlying the Middle(?) Triassic kaolinitic sandstones in locality 16 (Góra Świętej Anny). Pebble *a*-axes show a prevalent NNW–SSE orientation (see the inset rose diagram). **B.** Microscopic view of lithic sandstones from locality 34, composed of subangular quartz and feldspar grains (F; see inset close-up) cemented with siliceous matrix. Note the admixture of brown-greenish glauconite (gl.) and the hexagonal outline of largest quartz grains (Q), marked with arrows. **C.** Planar cross-stratified quartzose sandstones (facies Sp) at locality 32. **D.** Quartzose sandstones with planar cross-stratification (facies Sp) in a loose block at locality 35. Note the gravel facies GSm in the lower parts of individual cross-strata sets. **E, F.** *Ophiomorpha* isp. (*Oph.*) and *Thalassinoides*

respectively; Table 1 and Fig. 9). The cross-strata sets are up to 0.4 m thick and bounded by sharp, near-horizontal bases (Fig. 12B). Bioturbation structures are relatively rare, with solitary U-shaped escape traces and *Ophiomorpha* isp. noted in the middle part of the tor at locality 27. Present are coquina lags, preserved as concave-upwards casts and voids (facies GSc; Fig. 12B). The cross-stratified sandstones pass upwards into massive and slightly bioturbated sandstones (facies Sm and Sb, respectively) that form sharp-based beds up to 1 m thick in the top part of the tor (Figs 9, 12A).

The overlying, upper part of the Gorzeszów Member is well exposed at locality 31, where the outcrops show massive and bioturbated sandstones (facies Sm) with local poorly visible trough cross-stratification (facies St; Fig. 9). Primary stratification is strongly obscured by the erosional relief and surficial weathering of vertical tor surfaces. The lowermost parts of isolated tors in the SW part of the questa ridge show massive sandstones (facies Sm) with barely visible trough cross-stratification marked by grain-size changes (facies St/St₁; Fig. 12C). Cross-strata sets attain a thickness of 1 m and show strata dip towards the W and SW. The cross-stratified sandstones pass upwards into massive and locally bioturbated sandstones (facies Sm and Sb, respectively; Table 1 and Figs 9, 12D) with the beds up to 1.5 m thick, displaying sharp and undulating bases. The bed bases show a continuous lag of crushed shell debris including *Lima* sp. and *Pecten* sp. in convex-upwards, stable position and an admixture of scattered quartz granules up to 3 mm in size (facies GSc; Fig. 12E).

Above this horizon of facies Sm/Sb occur sandstones with relics of low-angle stratification, presumably of hummocky type (facies Su₁; Table 1 and Fig. 12D). These sandstones pass gradually upwards into massive, slightly graded and predominantly bioturbated sandstones (facies Sm₂ and Sb, respectively) that locally exhibit faint parallel cross-stratification dipping towards the SW, opposite to the tectonic dip. Bioturbation structures include straight or slightly curved vertical *Ophiomorpha* isp. (Fig. 12F) and U-shaped escape traces, as described by Wojewoda (1998b). The non-calcareous Gorzeszów Member sandstones pass upwards into calcareous deposits assigned herein to the Upper Heterolithic Series. The sedimentary contact between the Gorzeszów Member and Upper Heterolithic Series is unexposed, but cartographic evidence suggests a gradual upward transition with a decreasing content of the detrital grains and an increasing contribution of the matrix and calcareous cement.

The Upper Heterolithic Series (middle–upper Turonian). Calcareous, medium- to fine-grained sandstones and mudstones of the Upper Heterolithic Series (Fig. 3) overlie the Gorzeszów Member sandstones and occupy the central part of the KB (Fig. 8). From the base upwards,

the Upper Heterolithic Series includes calcareous sandstones passing upwards into mudstones and siltstones, followed by calcareous sandstones. The deposits are assigned to the middle–upper Turonian and reach a thickness of up to 30 m along the axis of the KB.

The lowermost part of the Upper Heterolithic Series consists mainly of fine- to medium-grained, light to dark grey calcareous sandstones with mudstone and siltstone intercalations up to 10 cm thick. The sandstones are well exposed at locality 23 (Fig. 13A), as well as in small outcrops in the Zadrna river valley in the village of Jawiszów. They are poorly to moderately well sorted and composed mainly of poorly rounded detrital quartz grains, 0.1 to 0.2 mm in size, occasionally up to 0.5 mm (Fig. 13B). Quartz detritus constitutes up to 65% of the grain framework, with the rest comprising partly kaolinized feldspar grains (up to 10%), lithic grains of metamorphic and subordinate igneous rocks (up to 5%) and bedding-parallel accumulations of mica flakes. A small admixture of glauconitic grains and scattered bioclasts (foraminifer tests) was also observed. The sandstones are cemented mainly by sparite crystals, 0.05 to 0.1 mm in diameter, and subordinately by a brownish micritic or clayey matrix. Numerous concretions and irregular nodules occur within beds with an increased carbonate content.

Similarly as in the Lower Heterolithic Series, the lowermost part of the Upper Heterolithic Series consists of massive, macroscopically structureless, pale- to dark-grey, fine-grained and strongly fractured sandstones and sandy mudstones (facies Sm/FSm, respectively; Table 1 and Figs 9, 13A). The individual beds are mainly up to 0.5 m thick, but partially amalgamated. Relics of horizontal or subhorizontal stratification marked by minor changes in sand grain size are occasionally recognizable. The relic strata locally are gently undulating in the lowermost parts of beds, especially at locality 23, probably representing hummocky stratification (facies Su₁; Fig. 13A, C). Sharp and possibly erosional bases of the sandstone beds may support this interpretation. The faintly stratified sandstones pass upwards into bioturbated and massive sandstones (facies Sm/SFm and Sb/SFb, respectively; Fig. 13D) with numerous vertical or curved *Ophiomorpha* isp. and rare body fossils. Macroscopic accumulations of crushed shells (fragments of up to 2 cm in size) were observed within rock blocks fallen off the outcrop. Dissolved bivalve shells in life position were noted in the middle part of the succession exposed at locality 23.

The Upper Jointed Sandstone (Krzyszów Member, upper Turonian–lower? Coniacian). The Upper Jointed Sandstone, assigned herein to the Krzyszów Member (Fig. 3), is exposed in the central part of the KB, between

isp. (*Th.*) on the lower surfaces of quartzose and lithic sandstone beds ca. 1 m above the Triassic-Cretaceous unconformity at localities 34 and 16, respectively. **G.** Massive sandstones (facies Sm) with sharp erosional boundaries capped by shell debris in the form of lens-shaped clusters (facies GSc) at locality 37 (Libna quarry). Note the relic hummocky stratification (facies Su₁) above shell lag (marked by white dotted lines) passing upwards into normal-graded sandstones (facies Sm₂). **H.** Shell lag (facies GSc) containing chaotically arranged scaphopod moulds of *Dentalium sexcarinatum* at locality 33. **I, J.** Wood fragments with casts of bivalves boring *Teredolites clavatus* (*Ter.*) in a loose sandstone block at locality 37 (Libna quarry).

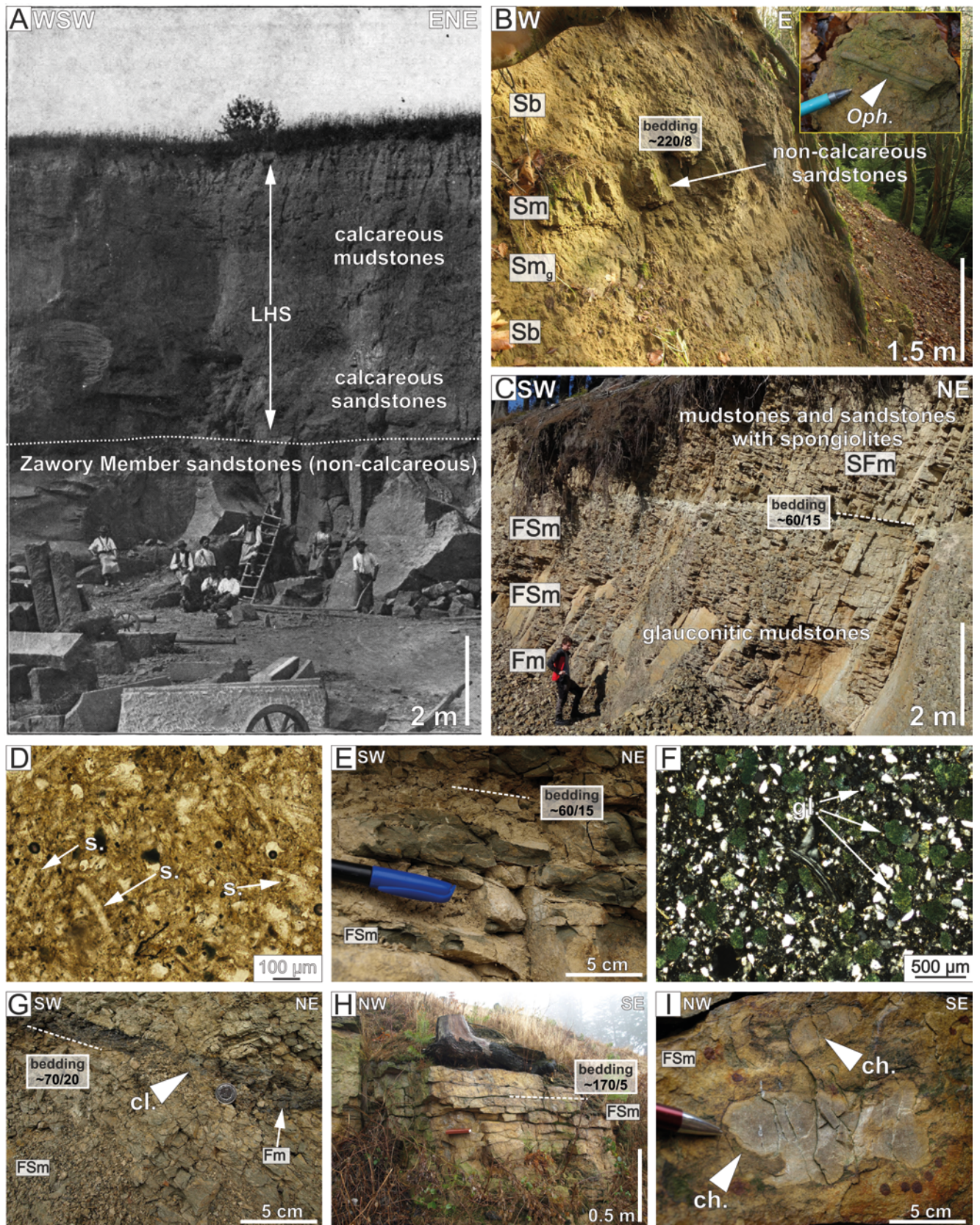


Fig. 11. Sedimentary features of the Lower Heterolithic Series in the Krzeszów Brachysyncline. **A.** Historical photograph from the Łączna quarry (from Flegel, 1904; locality 36, presently unexposed) showing vertical transition from the lithic sandstones of the Zawory Member (photograph bottom) to the calcareous sandstones and mudstones of the Lower Heterolithic Series (photograph top). Note the corresponding upward change in the degree of sandstone weathering and fracturing. **B.** Strongly weathered and fractured, bioturbated and normal-graded calcareous sandstones (facies Sb and Sm, respectively) above the Zawory Member sandstones at locality 37. Note the interbeds of non-calcareous massive sandstone (facies Sm_g; see arrow) and *Ophiomorpha* isp. (*Oph.*) in calcareous sandstones (see inset close-up). **C.** Non-calcareous, strongly fractured massive glauconitic mudstones (facies Fm/FSm) passing upwards into siliceous

the villages of Krzeszów and Jawiszów (Fig. 8). Due to their weak cementation, the sandstones used to be mined as quartzose, moulding sand in a large, presently flooded quarry in Krzeszów. At present, the sandstones crop out only in the upper parts of the quarry walls (localities 24 and 25) and as an erosional outlier, 120 × 50 m in size and up to 12 m high (locality 26), referred to earlier as Dachs Berg (Scupin, 1935; Berg and Dathe, 1940). Therefore, the Krzeszów Member sandstones cropping out in the KB were earlier termed the Dachsberg Sandstones (Ger. Dachsberg Quader; cf. Scupin, 1935). Indistinct sections of the lowermost part of the sandstones are also exposed in Krzeszów village, along the road linking Krzeszów and Krzeszówek (locality 19).

The Krzeszów Member sandstones are weakly cemented, poorly to moderately sorted, whitish to light grey, medium-grained quartzose arenites, with granule-rich intercalations, especially in the lowermost part of the succession. The grain framework is predominantly subangular to subrounded quartz detritus (up to 98%) with strongly kaolinized grains of white feldspar (locally up to 10%) and subordinate mica and lithic grains. Grains with diameters at 0.2–0.5 mm dominate, but in the lowermost part of the profile, occur scattered quartz granules up to 3 mm in size. The sandstones contain a white, clay-siliceous cement, locally with a high content of kaolinite matrix.

The lowermost part of the Krzeszów Member exposed at locality 19 contains coarse-grained sandstones showing planar angular cross-stratification and subordinate trough cross-stratification (facies Sp and St, respectively; Figs 9, 14A, B). The vertically stacked cross-strata sets have uniform thicknesses of up to 0.2 m and nearly horizontal bases lain with thin (up to 3 cm) gravel units containing granules up to 0.5 cm in size. Strata foresets show high-angle (30–35°) inclination towards the SSE (Fig. 14A). In the small abandoned quarry in Krzeszów (locality 19), facies Sp passes upwards into facies St) with bioturbation structures occurring as single, vertical or subvertical *Ophiomorpha* isp. with diameters of 5 mm, reaching down to 10 cm depth (Fig. 14B). The bedding surface of one block at locality 19 is covered by patches of burrows, probably *Thalassinoides* isp. No body fossils were found within the Krzeszów Member in both this and earlier studies (Jerzykiewicz, 1971).

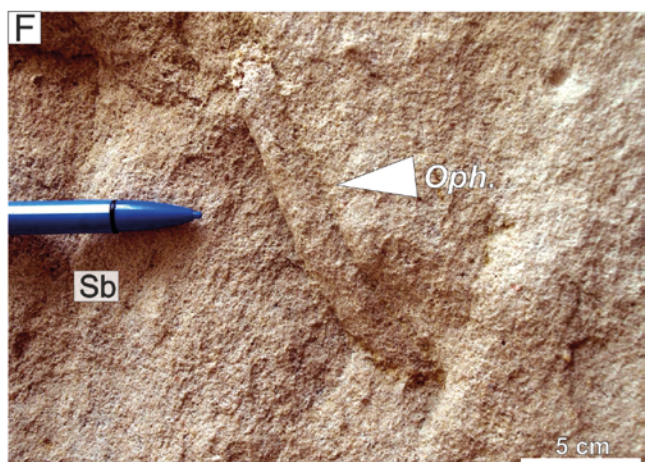
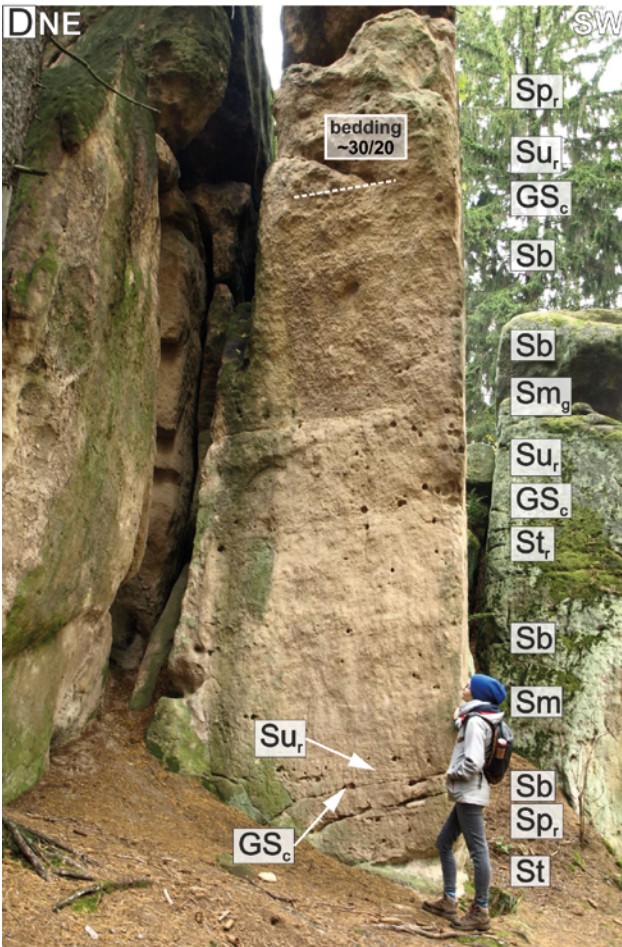
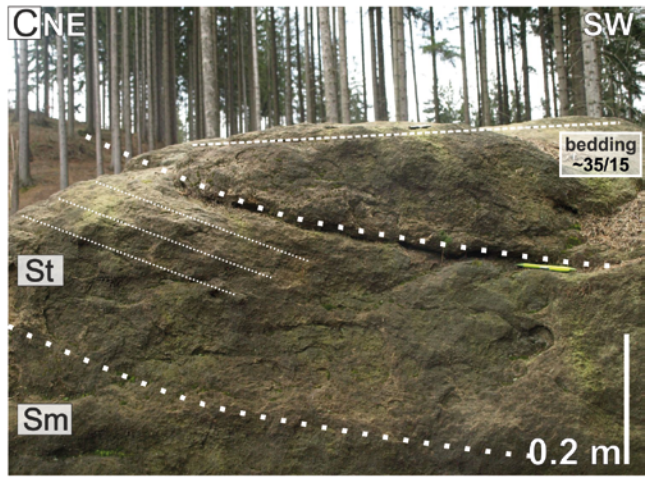
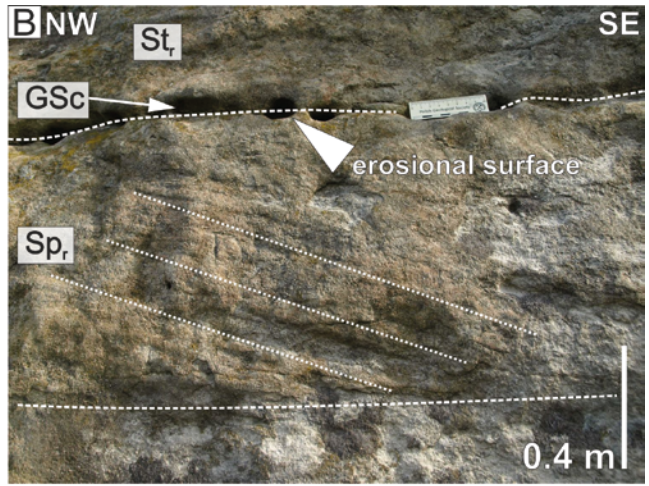
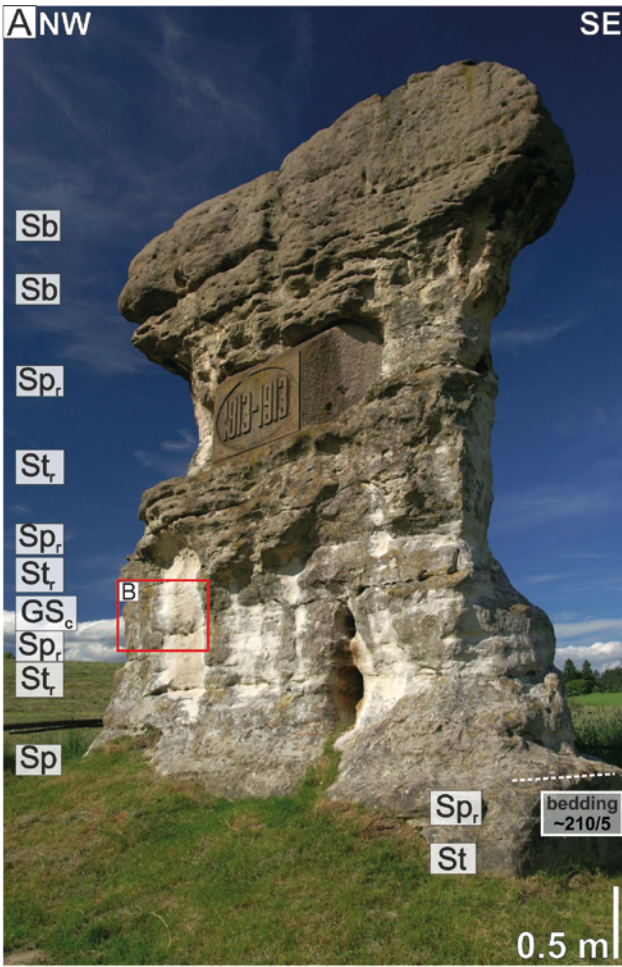
The middle and upper part of the Krzeszów Member in an abandoned sand pit in Krzeszów (localities 24/25) show planar tangential cross-stratification with strata sets 0.8 to 1.5 m thick, sharp-based and extending laterally for several metres (facies Sp₁; Table 1 and Fig. 14C, E). Foreset dip directions are towards the S and SSE (Fig. 9). In the eastern wall of the pit (locality 26), the cross-stratified sandstones are underlain by a massive, bioturbated sandstone bed up to 0.5 m thick (facies Sb; Figs 9, 14C) and pass further

upwards into trough cross-stratified sandstones (facies St) with strata sets up to 0.3 m thick. They are exposed in the uppermost part of the pit, as well as an isolated trending NNW–SSE at locality 26 (Fig. 14D). The foresets with common reactivation surfaces dip to the S and SE, but locally towards the N and NW, showing weakly bimodal orientation. Solitary *Ophiomorpha* isp. occurs locally. The top of the tor corresponds to the present-day subaerial (erosional) exposure and at the same time constitutes the topmost part of the Cretaceous succession in the KB area.

Environmental interpretation

Coarse-grained facies. This integrated cartographic and sedimentological study shows that the early Late Cretaceous sedimentation in the WG and KB areas at the NE fringe of the Bohemian Massif involved a range of shallow-marine depositional environments, as is typical of the epicontinental Upper Cretaceous within and around the Bohemian Massif (e.g., Milewicz, 1997; Wojewoda, 1997; Uličný, 2001; Uličný *et al.*, 2009a; Leszczyński, 2018; Leszczyński and Nemeč, 2020). The clast-supported conglomerates (facies Gm/GSm and Gm_g/GSm_g), referred to as the “basal conglomerates”, occur in the lowermost part of the Cretaceous succession in both study areas. These gravelly deposits are interpreted as a transgressive, strongly winnowed lag related to an in-place reworking of the pre-Cretaceous substrate. This process was probably due to wave action and current-induced erosion during the late Cenomanian transgression. Vigorous, storm-generated and/or (?) tide-induced currents are evidenced by both shell debris (facies GSc/SGc; Table 1) and high mineralogical maturity of the conglomerates. The admixture of lithoclasts derived from the metamorphic bedrock in the southern part of the WG area supports the notion of an in-place substrate reworking with limited bedrock erosion and high-rate sediment evacuation. Although Gorczyca-Skała (1977) interpreted the transgressive deposits from the southern part of the WG as a “deposit of an abrasion platform which developed along a cliff built of metamorphic rocks”, there is no evidence to support this hypothetical notion. The orientation of pebble *a*-axes at the individual localities in both study areas indicates their probable alignment parallel to flow of marine currents, which would mean in-place pivoting of least mobile clasts (cf. Potter and Pettijohn, 1963; Harms *et al.*, 1975; Adamovič, 1994). The clast fabric points to an NNW–SSE current paths in the KB area and a NE–SW palaeotransport direction in the WG area. These transport directions are consistent with the palaeocurrent directions measured in the overlying Lower Jointed Sandstone (Figs 4A, 8). Bioturbation structures, such as solitary *Ophiomorpha* isp. within and below the transgressive lag, seem to support the notion of a high

mudstones and fine-grained sandstones with spongiolites (facies SFm) at locality 30. Photograph courtesy of J. Wojewoda. **D.** Microscopic view of siliceous mudstones composed mainly of dispersed and recrystallized detrital quartz grains and chalcedony sponge spicules (s.) cemented with recrystallized silica; locality 17. **E, F.** Macro- and microscopic views of glauconite-bearing, siliceous mudstones (“glauconitic horizon”; facies FSm) with visible dispersed nodules and aggregates of glauconite (gl.); locality 17. **G.** Black clay intercalation (cl.) with a high content of organic matter within glauconite-bearing, strongly fractured, massive siliceous mudstones (facies FSm); locality 30. **H, I.** Outcrop and close-up view of siliceous mudstones and fine-grained sandstones (facies Fm/FSm) with brown chert nodules (ch.) at locality 17.



sediment evacuation and low accumulation rate (Nádaskay and Uličný, 2014).

The overlying, cross-stratified quartzose sandstones (facies Sp and St) in the lowermost part of the Wilków Member and Zawory Member, with their high mineralogical and textural maturity, indicate transport of well-washed sand in the form of migrating 2D and 3D dunes driven by unidirectional currents (Table 1; e.g., Allen, 1982; Ashley, 1990; Collinson and Mounthey, 2019). The predominance of sand with

cross-set thicknesses below 3 m indicate an upper shoreface bathymetry in the two studied structural marine passages, apparently tectonically-controlled straits. The cross-strata reveal opposite transport directions, towards the W and NW in the WG strait and towards the SE in the KB strait, which may reflect a hydrodynamic ‘watershed’ for tidal currents within the Sudetic seaway linking the Tethys and Boreal provinces (cf. Dalrymple, 1984; Davis, 2012; Longhitano, 2013; Collinson and Mounthey, 2019; Leszczyński and Nemeč, 2020).

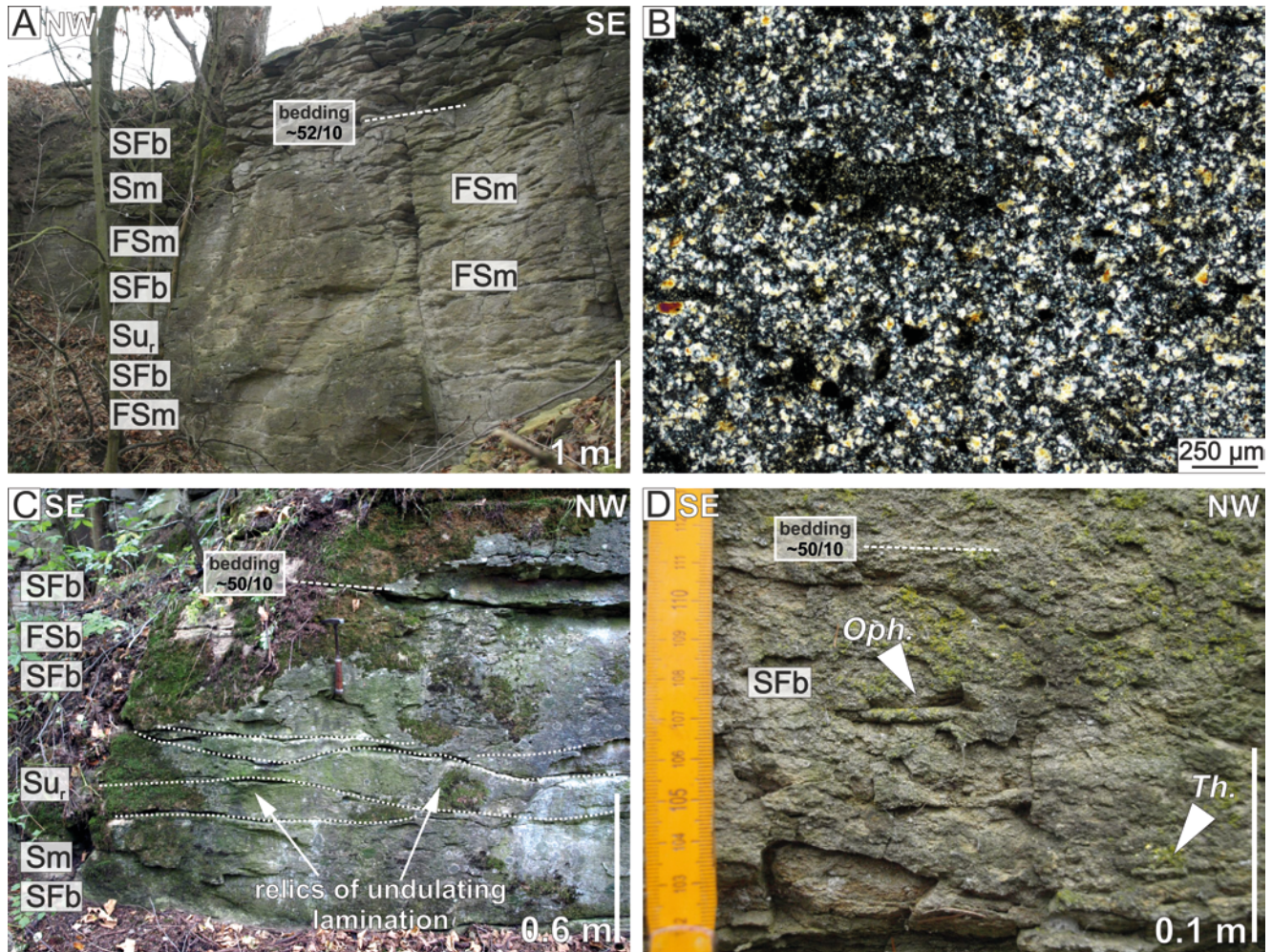


Fig. 13. Sedimentary features of the Upper Heterolithic Series in the Krzeszów Brachysyncline. **A.** Massive and bioturbated fine-grained calcareous sandstones (facies Sm/Sb) and sandy mudstones (facies FSm/FSb) with relic hummocky stratification (facies Su) at locality 23 (abandoned Jawiszów quarry). **B.** Microscopic view of sandy calcareous mudstone composed mainly of strongly recrystallized detrital quartz grains cemented by micrite; locality 23. **C.** Lenticular packages of fine-grained sandstones with relic gently undulating stratification, probably of hummocky type (facies Su), in a vertical outcrop section at locality 23. **D.** Bioturbated calcareous fine-grained sandstones (facies SFb) with solitary *Ophiomorpha* isp. (*Oph.*) and *Thalassinoides* isp. (*Th.*) at locality 23.

Fig. 12. Sedimentary features of the Gorzeszów Member sandstones in the Krzeszów Brachysyncline. **A.** Lower part of the Gorzeszów Member subarkosic sandstones exposed in the Diabelska Maczuga (Devil’s Club) tor at locality 27. Sandstones with poorly visible planar cross-strata (facies Sp) and subordinate trough cross-strata sets (facies St) are overlain by massive or slightly bioturbated sandstones (facies Sm/Sb) at the tor top. **B.** Close-up view of the tor middle part with relic planar cross-stratification in sandstones (facies Sp) overlain by coquina lag horizon (facies GSc). **C.** Trough cross-stratified sandstone (facies St) in the lower part of the Gorzeszowskie Skály section (locality 31), with cross-strata dip to the SW. **D.** Middle part of the Gorzeszowskie Skály section (locality 31), showing massive or normal-graded sandstones (facies Sm/Sm) and bioturbated sandstones (facies Sb) with sharp or undulating bases covered with crushed shell debris (facies GSc). Above the shell lag occurs relic hummocky stratification (facies Su). **E.** Continuous shell lag (facies GSc) with crushed shells of *Lima* sp. and *Pecten* sp., in a loose sandstone block at locality 31. **F.** Single *Ophiomorpha* isp. (*Oph.*) in a bioturbated sandstone (facies Sb) at locality 31.

The lithic and glauconitic sandstones of the Wilków Member and Zawory Member form massive, normal-graded beds with relic cross-stratification and with repetitive horizons of disarticulated shell debris and gravel lags (facies GSc), bounded by undulating erosional bases and passing upwards into hummocky-stratified sandstones (facies Su/Su₁) or sandstones with trough and planar cross-stratification

(facies St and Sp). These facies are attributed to storm-enhanced tidal currents (Table 1). Fragmented shells with admixed granules, locally in the form of continuous debris horizons (facies GSc/SGc) are interpreted as storm-generated lags marking strong erosion and winnowing of sand-sized particles (cf. Clifton, 2005). The hummocky-stratified sandstone beds reflect storm-induced hydraulic

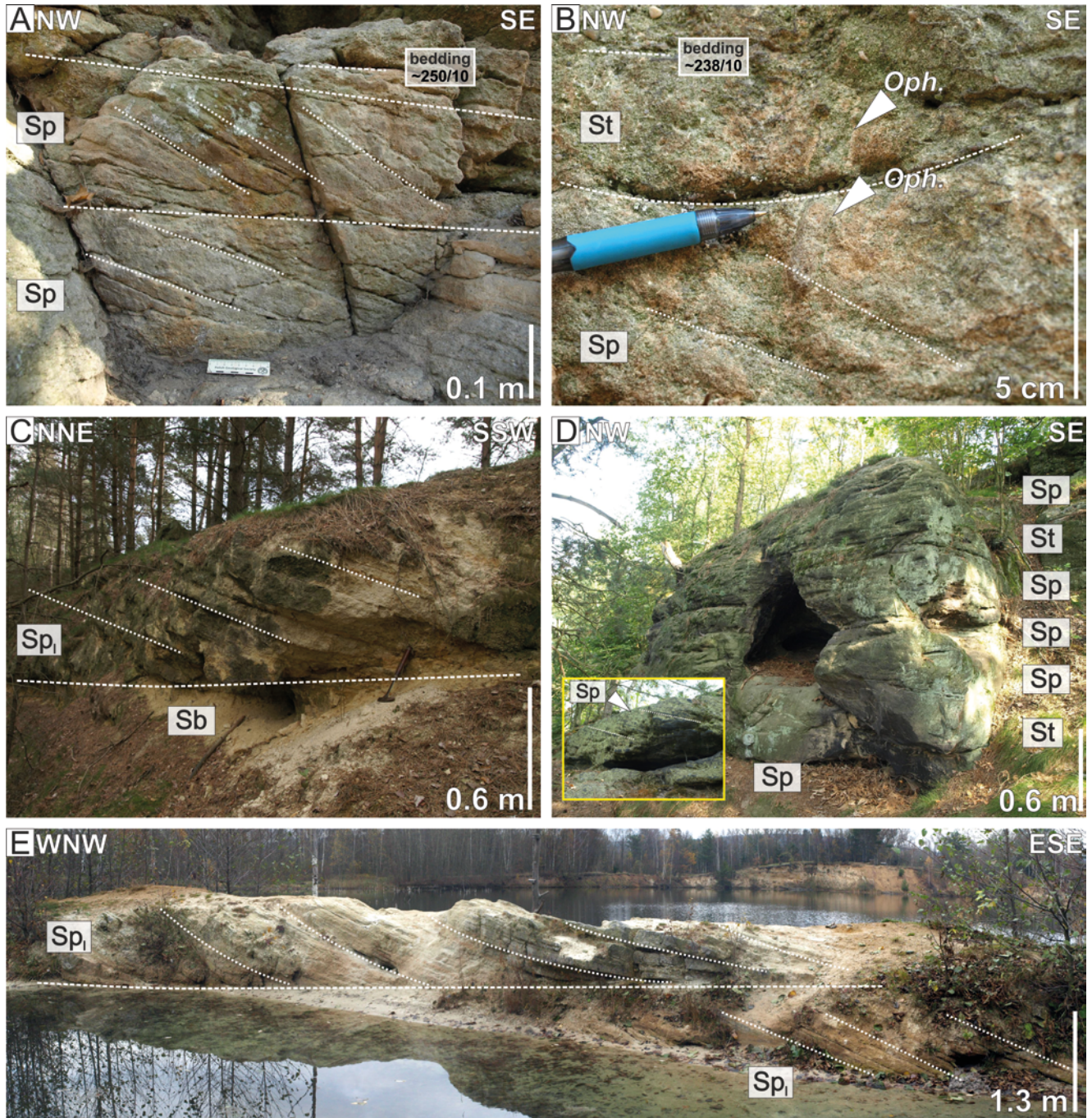


Fig. 14. Sedimentary features of the Krzeszówek Member sandstones in the Krzeszów Brachysyncline. **A.** Sandstones with planar angular cross-stratification (facies Sp) at locality 19. **B.** Solitary, nearly vertical *Ophiomorpha* isp. (*Oph.*) in a cross-stratified sandstone at locality 19. **C.** Planar tangential cross-stratified sandstone (facies Sp₁) with foresets inclined to the S and SSE, underlain by a massive, bioturbated sandstone bed (facies Sb) at locality 25 (Krzeszówek sand pit). **D.** Isolated sandstone tor at locality 26 (Ger. *Dachs Berg*) showing vertically stacked planar and trough cross-strata sets (facies Sp and St; see inset close-up) with weakly bimodal palaeocurrent directions to the S/SE and subordinately to the N/NW. **E.** Planar tangential cross-stratified sandstones (facies Sp₁) with foresets inclined to the S/SSE at locality 24 (Krzeszówek sand pit).

combined-flow regime (e.g., Harms *et al.*, 1975; Dott and Bourgeois, 1982; Reading and Collinson, 1996). Local wave-rippled sandstone layers (facies Srw) are probably a result of the declining storm-wave action. The frequency of storm-related beds decreases upwards, where massive or strongly bioturbated sandstones prevail (facies Sm and Sb), which may reflect strait shallowing due to sediment aggradation, with the collapsing of tide-driven flow bedforms, *in-situ* sediment liquefaction and local sand dumping from overcharged tidal currents (Leszczyński, 2018; Collinson and Mountney, 2019). The uppermost, strongly bioturbated massive sandstones were deposited above the fairweather wave base once the flow intensity of tidal currents in the shallowing straits had markedly declined.

The Wilków Member and Zawory Member share their facies range with the Gorzeszów Member sandstones in the KB area. Erosional-based units with continuous shell lags and relic hummocky stratification occur at locality 31 and are interpreted as tempestites (Reading and Collinson, 1996). The overlying massive sandstones are a result of bioturbation (facies Sb). Isolated cross-strata sets (facies Sp and St) in the lower part of the Gorzeszów Member represent basinwards-migrating littoral sand dunes, possibly storm-driven or tidal. The palaeocurrent data from the Gorzeszów Member in the KB area and from the uppermost part of the Wilków Member in the WG area indicate transport towards the SW and W, nearly perpendicular to the basin axis.

The dune-scale cross-strata sets in the sandstones of the Zawory Member and Krzeszów Member in the WG and KB areas are oriented parallel to the basin axis and interpreted as vertically stacked tidal dunes (e.g., Belderson *et al.*, 1982; Ashley, 1992; Johnson and Baldwin, 1996; Longhitano and Nemeč, 2005; Davis, 2012). The majority of cross-strata sets up to 0.3 m thick, but thicker sets (facies Sp) are observed in the KB area (Fig. 14). Jerzykiewicz (1968) described planar cross-strata sets up to 3 m thick from localities 24 and 25. They probably represent tidal transverse bars/sandwaves (cf. Allen, 1982; Dalrymple, 1984; Davis, 2012) or are due to the dune height growth by overstepping (Leszczyński and Nemeč, 2020). The lack of storm- and wave-induced structures indicates deposition below the fairweather wave base. Unidirectional palaeocurrent pattern predominates at the individual localities and is rarely bidirectional on an isolated outcrop scale (e.g., locality 26 in the KB), but is recognizably bipolar on a regional scale (Figs 4A, 8). Similar patterns characterize many narrow, tectonically controlled marine straits (e.g., Longhitano and Nemeč, 2005; Longhitano, 2013). The dominant palaeocurrent directions in the Upper Jointed Sandstone are towards the WNW and NW in the WG strait and towards the SSE and S in the KB strait. This may resemble the pattern of tidal-current circulation in the modern Messina Strait (Longhitano, 2013) – where an across-strait structural ridge acts as a ‘watershed’ sill dividing the directional action of tidal currents.

Fine-grained facies. The fine-grained facies occurring between the non-calcareous sandstone lithosomes in both study areas are interpreted to have been deposited in the lower shoreface to offshore zone (*sensu* Reading and Collinson, 1996).

The general lack of wave-formed structures in the mudstone-rich facies SFm/Fm (Table 1) of the Heterolithic Series in the WG area indicates deposition below the storm wave base (e.g., Reading and Collinson, 1996). Likewise, the strong bioturbation of mudstone facies SFb/Fb reflects quiet water conditions. Facies SFm/Fm were deposited probably from fine-grained suspended load spread seawards by storm-generated currents (e.g., Valečka, 1984; Table 1), as indicated by the abundance of crushed shells. Intercalations of fine- and medium-grained massive sandstones (facies Sm) in the lower and uppermost parts of the Heterolithic Series in the WG area may represent episodic incursions of storm-derived sand (e.g., Reading and Collinson, 1996).

The massive, partly bioturbated calcareous sandstones of the Lower Heterolithic Series in the KB area are interpreted as deposits of the lower shoreface to offshore transition zone characterised by repetitive variation of high- and low-energy conditions. The massive structure of calcareous fine-grained sandstones and the overlying mudstones resulted from intense burrowing in low-energy offshore conditions. However, intercalations of massive or weakly graded sandstones noted in the Lower Heterolithic Series may be tempestites or represent storm-enhanced rip currents, as indicated by highly crushed bioclasts. Similar heterolithic deposits in the southern part of the Intra-Sudetic Basin (Stołowe Mountains) are interpreted as shallow-marine distal-most tempestites (Wojewoda, 1997; Rotnicka, 2005). The siliceous mudstones and spongiolites above the calcareous facies of the Lower Heterolithic Series are interpreted as deposited from suspension, reflecting low-energy, yet relatively well-oxygenated offshore conditions with no evidence of wave or current activity. A low rate of sediment supply is confirmed by the significant increase in the content of authigenic glauconite, especially in the so-called glauconitic horizon within siliceous mudstones (gaizes). According to the earlier palaeogeographic reconstructions, these deposits correspond to the greatest bathymetry, sediment starvation and maximum relative sea-level rise in the Intra-Sudetic Basin (Wojewoda, 1997).

Possible storm-generated structures, although poorly preserved, occur in the fine-grained calcareous sandstones of the Upper Heterolithic Series. The beds have sharp, erosional bases, bear strongly disarticulated bioclasts and show faint hummocky stratification. They are thought to be distal tempestites, deposited in the lowest shoreface to offshore transition zone. The homogeneous, strongly bioturbated sandstones and mudstones capping the storm beds and bearing moulds of bivalve shells in life position are considered to represent low-energy offshore conditions. Palaeocurrent directions in the overlying, weakly cross-stratified sandstones are similar as in the Gorzeszów Member sandstones, towards the SW (Fig. 8).

DISCUSSION: SEDIMENTARY ENVIRONMENTS AND PALAEOGEOGRAPHIC DEVELOPMENT

The WG and KB marine palaeostraits are important parts of the ‘missing link’ within the Late Cretaceous Sudetic

seaway connecting the Tethyan and Boreal provinces. The lateral and vertical facies variation recognised in the WG and KB areas reveal a differing response of these primary sub-basins to eustatic sea-level changes and point to a strong influence of regional tectonics. The Late Cretaceous marine transgression coincided with the European culmination of the Alpine orogeny, which affected also the Bohemian Massif and its surroundings. The palaeoenvironmental interpretation of the WG and KB in the present study differs significantly from the earlier, simplistic palaeogeographic schemes proposed for these areas. The difference includes the range and hydrodynamic interpretation of sedimentary facies, as well as the spatial-temporal palaeogeographic changes within the Sudetic seaway.

The non-calcareous sandstone lithosomes overlain by calcareous sandstone to mudstone facies are stratigraphically arranged into fining-upwards transgressive depositional cyclothem, with sand-dominated nearshore deposits passing into mud-dominated offshore deposits. The lack of a precise biostratigraphic dating of the succession renders it difficult to speculate as to how much of this cyclicity is eustatic (cf. Haq, 2014 and Fig. 3) and how much due to regional tectonism. The WG and KB marine straits were tectonically subsiding features, whose interconnection was increasingly affected by tectonic inversion – with a transverse structural divide first making a directional “watershed” for tidal current hydrodynamics and eventually separating the two strait segments by a dome-like uplift.

The late Cenomanian marine sedimentation was preceded by a period of intense weathering and peneplaining of a low-relief terrane of the Sudetic Block since the Middle Triassic until the mid-Cretaceous. After this period, the central Europe was flooded by the Cenomanian epicontinental sea, as reflected in the base-Cretaceous unconformity (Uličný *et al.*, 2009b). According to the existing palaeogeographic reconstructions, a system of shallow-marine straits developed between the North Sudetic and Intra-Sudetic basins, including the WG and KB passage. It is generally accepted that this marine Sudetic seaway was bounded by an archipelago of emerged landmasses – the East Sudetic Island to the E/NE and the West Sudetic Island to the W (Scupin, 1913, 1936; Andert, 1934; Milewicz, 1997). It is also accepted that these adjacent landmasses acted as the principal source areas for the Sudetic seaway (Jerzykiewicz and Wojewoda, 1986; Milewicz, 1997; Wojewoda, 1997; Uličný, 2001; Leszczyński, 2018; Leszczyński and Nemeček, 2020), even though the KB–WB strait system was chiefly a sediment transfer zone. The main accumulation of sediment occurred in the Intra-Sudetic and North Sudetic basins at the opposite termini of the strait system.

The KB and WB features are present-day structural relics of wider primary straits, as indicated by their pattern of sediment transport direction and offshore-transition tempestites implying considerable storm-wave fetch. The frequency of storm layers in nearly in all outcrops decreases upwards, which seems to indicate a decreasing wave fetch and probably narrowing of the strait system. Palaeotransport directions overall indicate bidirectional NW–SE tidal currents (Fig. 15A) combined with the storm-wave action and probable wind-generated alongshore currents. Intense wave action

is reflected in the high textural maturity of the quartzose sandstones in both the WG and KB areas. The southernmost part of the WG area could have been a narrow strait-centre zone (*sensu* Longhitano, 2013; Fig. 15A), maximising the action of tidal currents, as suggested by the maximum accumulation of coarse-grained sediment (e.g., localities 13 and 15). The topography of this strait segment was probably inherited from the Early Triassic structural configuration (cf. Kowalski, 2020a). There is no sedimentological evidence of an erosional coastal cliffs in the southern part of the WG (near the hypothetical West Sudetic Island), as suggested by Gorczyca-Skała (1977). The WG strait became colonized by a seafloor-burrowing assemblage of low-diversity benthic organisms, right from the basal transgressive lag. Their burrows are dominated by *Ophiomorpha* isp. and *Thalassinoides* isp.

The latest Cenomanian sedimentation in the KB segment was dominated by fine-grained deposits, sandy to muddy, representing an alternation of lower shoreface to offshore conditions (Fig. 15B), with strong bioturbation and episodic storm-wave influence. Notable in the Lower Heterolithic Series in the KB area is the abundance of siliceous cement in mudstones (gaizes), derived from the dissolution of sponge spicules. These deposits seem to reflect the greatest bathymetry of the axial part of the strait at a maximum sea-level stand (Wojewoda, 1997). A similar interpretation is given for the sandstones with chert nodules in the Orlice–Ždár area of the Bohemian Cretaceous Basin (Mitchell *et al.*, 2014), considered to represent the “most basinward extension of coarse-grained clastic depositional system”. Notably, siliceous mudstones and gaizes are lacking in the WG strait segment (Fig. 4A), where their time-equivalent are the late Cenomanian coarse-grained lithic sandstones of the Wilków Member. This facies difference and the greater thickness of the Wilków Member lithosome (up to 37 m), as compared to that of the Zawory Member in the KB (up to 10 m), indicate a greater subsidence in the (fault-bounded?) WG strait segment and perhaps a different local basin-floor configuration. The strait axial depocentre there probably corresponded to the axis of the present-day WG, which acted as a distinct tectonic trough since the early Permian (Kowalski *et al.*, 2018) and might have had a higher rate of subsidence than the KB in both the Triassic (Kowalski, 2020a) and Late Cretaceous. The Cretaceous KB strait segment may have been shallower or its present-day narrow structural axis may not correspond to the Late Cretaceous strait axial zone (Fig. 15B). Palaeocurrent data show that the coarse-grained siliciclastic sediment there was probably derived from the East Sudetic Island area. The late Cenomanian palaeocoastline of the East Sudetic Island is uncertain, but may have been at the western margin of the present-day Góry Sowie Massif, ca. 15 km to the east of the KB strait (cf. Radwański, 1975; Fig. 15B).

Marine offshore conditions prevailed in both study areas in the late early Turonian, probably due to eustatic sea-level rise (Figs 3, 15C; Haq, 2014). This caused sediment starvation followed by deposition of widespread calcareous muddy facies from suspension (hypopycnal plumes?) in low-energy settings, predominantly below the storm wave base. The influence of storm-generated and tidal currents

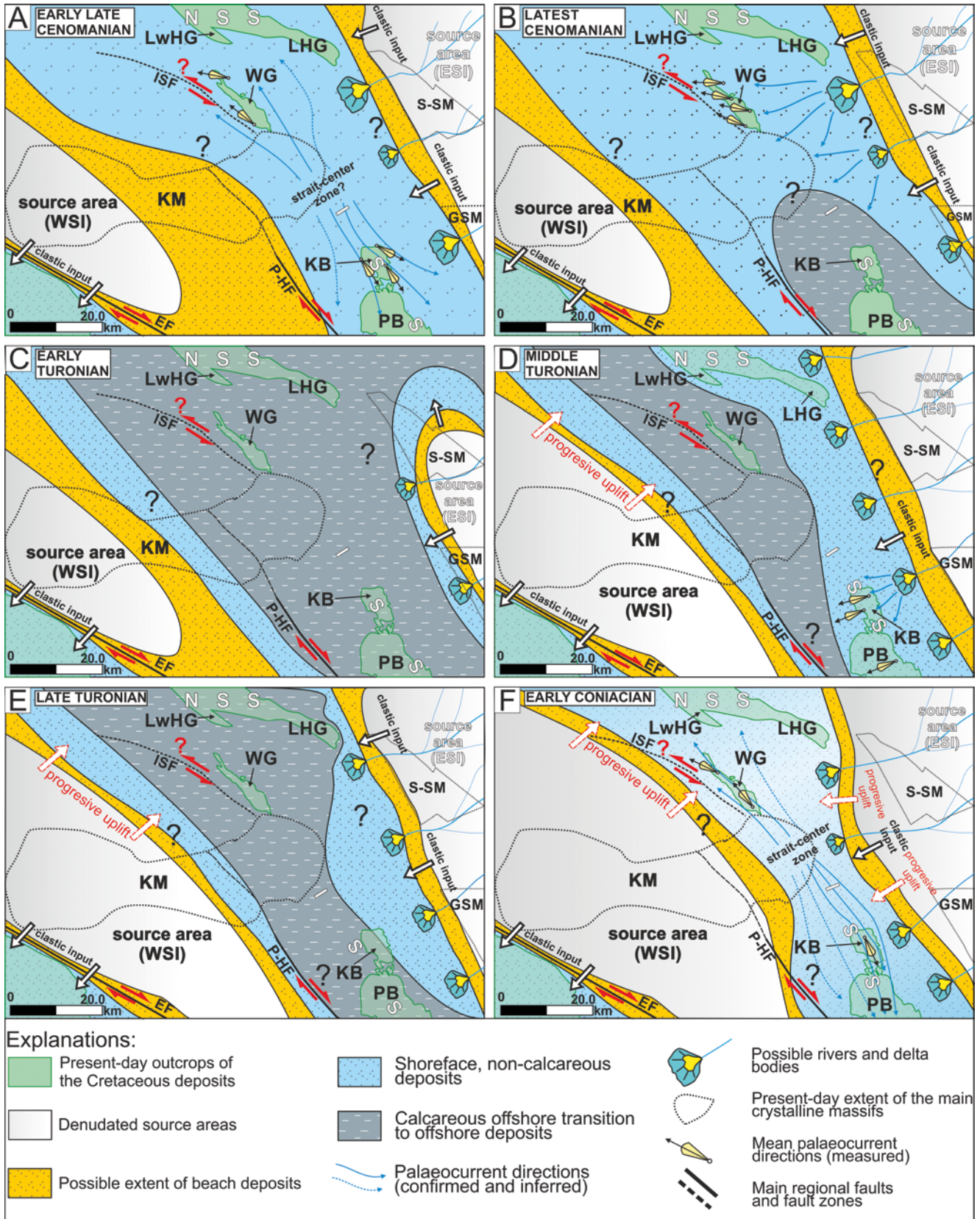


Fig. 15. Schematic palaeogeographic evolution of the North Sudetic and Intra-Sudetic basins in the early Late Cretaceous, from the late Cenomanian to early(?) Coniacian. Note the sediment source areas (“Sudetic Islands”) and presumed extent of their shorelines. The hypothetical sense of movement in the regional fault zones in the Late Cretaceous is after Aleksandrowski (1995), Uličný (2001) and Wojewoda (2007). For discussion, see the text.

decreased, while strong bioturbation occurred. The main landmasses in the early Turonian were characterised by a low relief and their shorelines were situated far away from the strait axis (Fig. 15C).

In the middle Turonian, the southern segment of the sea-way – corresponding to the present-day KB – became progressively filled with coarse-grained siliciclastic sediment supplied from the East Sudetic Island (Fig. 15D). This is indicated by the basinward thinning of the Gorzeszów Member lithosome towards the W and NW between the Lower Heterolithic Series and Upper Heterolithic Series (Fig. 3) and by offshore-directed palaeocurrents (Figs 8, 9). Cross-strata sets in the lower part of the Gorzeszów Member reflect basinward migration of the 2D and 3D dunes. There is no evidence of basin-margin Gilbert-type deltas, although such features were reported from the coeval, middle Turonian sandstones (Jížera Formation) in the Broumov Cliffs ca. 15 km to the SE in the Czech part of the Intra-Sudetic Synclinorium (Police Brachysyncline; Uličný, 2001; Uličný *et al.*, 2009a). The lack of strait-margin foreshore deposits and deltas in the KB area may reflect larger distance from the shoreline of the East Sudetic Island (Fig. 15D). It cannot be precluded that the terrigenous sediment was supplied to the Intra-Sudetic Basin from the East Sudetic Island via river mouths and shallow-water deltas and was redistributed by tidal and wind-generated alongshore currents, with the shoreline systems un preserved. Notably, the middle and upper parts of the Gorzeszów Member sandstones show storm-related erosional coquinas, gravel lags as well as relic hummocky stratification, which indicate combined-flow tempestites and hence a considerable wave fetch. According to Wojewoda (2003), such features may practically preclude a deltaic origin of the sandstones. Palaeotransport directions for the Middle Jointed Sandstone in the KB have been reconstructed for the first time in the present paper. The primary sedimentary structures were overlooked in the previous regional studies by Jerzykiewicz (1971), who suggested that “the bedding in the sandstones [...] cannot be identified with the stratification”.

The relative sea-level rise in the late middle Turonian resulted in renewed deposition of distal shoreface to offshore transition fine-grained sandstones and offshore mudstones in the KB area. Offshore conditions in the WG area prevailed during the early to early late Turonian (Fig. 15E). At the beginning of the early Coniacian, the area between the KB and WG possibly evolved into a narrowest strait zone dominated by transfer of coarse-grained siliciclastic sediment (Fig. 15F). Tidal currents could be amplified along this corridor, as inferred from the regional, bi-directional orientation of planar cross-strata showing reversing currents (Figs 4A, 8) and abundant reactivation surfaces. The areas of the present-day WG and KB most probably constituted a dune-bedded strait zone (*sensu* Longhitano, 2013) covered by 2D and 3D tidal dunes. The presence of tidal currents combined with alongshore drift in the NW segments of the North Sudetic Synclinorium area was indicated by el Bassyouni (1984), Wojewoda (1998a, c) and more recently by Leszczyński and Nemeč (2020). Regional-scale palaeocurrent analysis in the present paper is consistent with these interpretations. Mud drapes are widely considered as good

indicators of tidal environment (e.g., Johnson and Baldwin, 1996; Davis, 2012), and their lack shows that mud was kept by waves persistently in suspension (e.g., Longhitano and Nemeč, 2005). The increasing thickness of the Żerkowice Member and Krzeszówek Member sandstone lithosomes in both study areas may indicate an increased sediment supply, possibly due to a progressive uplift of the source areas since the middle Turonian (Fig. 15D–F).

The palaeotopography, spatial extent and hypothetical coastlines of the East and West Sudetic islands are poorly recognised and disputable. Until now, the WG area was palaeogeographically positioned close to the West Sudetic Island, corresponding to the Karkonosze-Izera and Lusatian massifs (Skoček and Valečka, 1983). However, the role of this landmass as a source area is perhaps recognizable only in the petrographic composition of the upper Turonian to lower Coniacian sandstones of the Żerkowice Member and Krzeszówek Member. There is also no palaeogeographic evidence the West Sudetic Island as an emerged landmass (palaeo-high) of crystalline rocks in the close proximity to the study areas during the early late Cenomanian to middle Turonian. The influence of this hypothetical landmass is not marked in the petrographic composition of the upper Cenomanian conglomerates and sandstones of the Wilków Member, which lack clastic material from the Karkonosze-Izera Massif. Only quartz grains with an admixture of large clasts were indisputably derived from the underlying metamorphic bedrock of the Kaczawa Metamorphic Complex (greenschists, chlorite schists and metacherts). Moreover, palaeotransport indicators in the upper Cenomanian to middle Turonian sandstones in the WG and KB show NE to SW directions as well as alongshore NW–SE directions, with no evidence of a NE-directed transport from the hypothetical West Sudetic Island located to the SW.

The increased thickness of upper Turonian to lower Coniacian sandstones in both study areas, coupled with their petrographic characteristics (i.e. high content of kaolinized feldspar grains and relatively low textural maturity of the sandstones), may indicate an increased subsidence and strait narrowing with an uplifted adjacent land area built of (weathered?) quartz-feldspatic granitic or gneissic rocks. Taking into account the late Turonian southeastern palaeotransport directions in the KB area, this may be the only premise indicating an emerged crystalline West Sudetic Island to the NW of the KB.

Such a palaeogeographic scenario is consistent with the provenance data of Biernacka and Józefiak (2009) and Biernacka (2012), who – based on heavy mineral assemblages from the central parts of the North Sudetic Synclinorium (middle Turonian Chmielno Member sandstones) – suggested that the present-day Karkonosze Massif (West Sudetic Island) “must have been covered by sediments in the Late Cretaceous and exhumed later than in the mid-Santonian” (Biernacka, 2012, p. 329). If that was the case, then areas adjacent to the Karkonosze-Izera Massif must have been also covered by older (Permian or Triassic?) post-Variscan molasse, which could have been redeposited since the late Turonian to Coniacian or even during the Santonian. The process of a late Turonian progressive uplift of the Karkonosze Massif is evidenced further by

the apatite fission track and thermochronologic data presented by Danišík *et al.* (2010). These authors point to a relatively rapid erosion of the Karkonosze Massif after the latest Turonian, which means that the crystalline massif was earlier covered by older post-Variscan deposits.

On the other hand, the presence of an uplifted and emerged land during the Late Cretaceous is well documented from the Lužice–Jizera sub-basin (NW part of the Bohemian Cretaceous Basin). The sub-basin was bordered by a landmass acting as the principal source area and called the West Sudetic Island (Uličný *et al.*, 2009a; Nádaskay and Uličný, 2014; Nádaskay *et al.*, 2019). The emerged area was located ca. 50 km towards the SW from the present-study areas. It seems, therefore, that the West Sudetic Island must have had a much smaller surface area than thus far considered (Fig. 15). The accelerated uplift of the West Sudetic Island area in the present-day Karkonosze–Izera Massif might have begun as late as in the late Turonian and Coniacian, and lasted to the Santonian, due to changes in the palaeostress field in the NE part of the Bohemian Massif (e.g., Malkovský, 1987). Earlier, the KB and WG would thus appear to be have been sourced directly from the East Sudetic Island.

The new findings of large, up to 0.6 m long, rafted wood fragments described in this paper from both the upper Cenomanian of the KB (locality 37) and the lower Coniacian of the WG (locality 14) point to the presence of emerged landmasses covered by vegetation, rather than submerged elevations, as suggested by Wojewoda (2003). Moreover, findings of the conifer plant *Dammarites albens* Presl in the southern parts of the KB (Łączna vicinity; Niebuhr, 2019) confirm the presence of emerged landmass in the nearest proximity of the study areas. These findings and their palaeogeographic importance are consistent with the palaeocurrent data presented in this paper and suggest that the floral remains must have been derived from the East Sudetic Island.

The KB and WG are presently separated by uplifted crystalline units devoid of Triassic–Cretaceous sedimentary rocks (Fig. 2). However, the two areas must have been at least periodically connected in the Early to Middle(?) Triassic (Kowalski, 2020a) and during the Late Cretaceous. Bidirectional palaeocurrent pattern indisputably indicates that the study areas must have been interconnected during the late Cenomanian and late Turonian/early Coniacian time (Fig. 15). Such a hypothetical connection has long been postulated (Partsch, 1898; Andert, 1934; Scupin, 1936), but remained unconfirmed by sedimentological evidence. There is no evidence in the northern part of the KB and the southernmost part of the WG to indicate isolated marine basins. The lack of Cretaceous deposits between the two study areas should rather be explained by their erosional removal due to the end-Cretaceous Alpine tectonic uplift.

There is no evidence of a tectono-eustatic isolation of the WB and KB outliers of the North Sudetic and Intra-Sudetic synclinoriums at least prior to the mid-Coniacian time. The North Sudetic Synclinorium remained open to the NW, but its SE part became increasingly paralic in the late Coniacian to Santonian (cf. Milewicz, 1997, 2006; Leszczyński, 2010, 2018; Leszczyński and Nemeč, 2020). The remnant Santonian deposits in the WG are

offshore-transition calcareous sandstones capping the non-calcareous Żerkowice Member sandstones at locality 14, which may suggest a KB–WG strait system reaching farther north, perhaps due to a differential tectonic subsidence within the latest Cretaceous Sudetic seaway. The Santonian record is incomplete, eroded at the tectonic inversion stage of the North Sudetic Basin in post-Santonian time (Solecki, 1994, 2011). The KB–WG strait branch suffered less inversion, as shown by its preserved relics, and the offshore transition environment therein may have been due to the late Coniacian marine transgression recognized in the North Sudetic Synclinorium (Leszczyński, 2010, 2018; Leszczyński and Nemeč, 2020). It seems that the North Sudetic Boreal embayment was linked with the Intra-Sudetic Tethyan embayment by at least two strait branches (Fig. 2): the Złotoryja branch, inverted in the mid-Coniacian and later erased by erosion (Leszczyński and Nemeč, 2020), and the WG–KB branch, inverted in the late Santonian and described in the present study.

CONCLUSIONS

The present study has integrated results of geological mapping, sedimentary facies analysis, new fossil-remain findings and latest borehole data to reconstruct for the first time the Wleń Graben and Krzeszów Brachysyncline strait system of the Late Cretaceous Sudetic seaway linking the Boreal and Tethys marine provinces. The study has shed new light on the Late Cretaceous palaeogeographic development at the NE fringe of the Bohemian Massif. The shallow-marine siliciclastic to calcareous facies are consistent with the epicontinental environment of the Bohemian Massif and its surroundings. No strait-margin foreshore or deltaic deposits have been found, which indicates strait width much greater than that of their present-day tectonic relics. Sedimentation in the WB and KB strait segment was coeval, from Cenomanian to at least early Santonian, but the regional diachroneity of their facies development points to an interplay of eustatic sea-level changes and local Alpine tectonism. Siliciclastic coarse-grained sandy sedimentation continued through the late Cenomanian in the WG area, but changed into a heterolithic to muddy sedimentation in the KB area.

The siliciclastic sandstone lithosomes overlain by calcareous heterolithic to muddy deposits formed fining-upwards transgressive depositional cycles, which may be eustatic or reflect pulses of tectonic subsidence. Facies diachroneity and a directional tidal-current ‘divide’ between the WG and KB suggest an important role of tectonic topography. The top of the Cretaceous succession in both study areas is erosional and corresponds to the present-day subaerial exposure.

Disputable is the role and palaeogeographic extent of the strait-bounding uplifted landmasses, known hypothetically as the West Sudetic Island and the East Sudetic Island. Facies analysis shows that the coastline of the West Sudetic Island must have been located much farther away from the strait system than previously assumed considered and probably corresponded to a structural block uplifted along the Main Lusatian Fault in the NW part of the Bohemian Cretaceous Basin. The KB–WB strait system seems to

have been sourced more directly from the East Sudetic Island, which probably corresponded with the present-day Góry Sowie Massif and Fore-Sudetic Block. The large rafted wood fragments with casts after wood-boring bivalves, along with previously described plant fossils in the KB area, indicate a vegetated landmass close to the strait system. Palaeocurrent data indicate derivation from the east.

The evidence of tempestites and storm combined-flow conditions indicates considerable wave fetch and supports the notion of a strait system width much greater than that of its present-day KB and WB tectonic relics. The wave action limited mud suspension fallout and was superimposed onto an axial NW–SE circulation of tidal currents with a regional bidirectional pattern.

Offshore transitional conditions prevailed in both study areas in the early Turonian, when the adjacent landmasses were probably largely inundated and their shorelines had shifted away from the strait system. In the middle Turonian, the southern (narrowest?) part of the KB strait segment was again filled with coarse-grained siliciclastic sediment supplied from the East Sudetic Island, probably due to local tectonic activity.

This multifaceted study as a whole contributes to a better understanding of the Late Cretaceous Sudetic seaway linking the Boreal and Tethyan provinces, and contributes to the existing knowledge on the palaeogeography and palaeoenvironments at the NE fringe of the Bohemian Massif.

Acknowledgements

The research was partly funded by projects nos. 0420/2285/17 and 0420/2678/18 of the Institute of Geological Sciences, University of Wrocław. I am grateful to Jurand Wojewoda (University of Wrocław) for numerous discussions during the preparation of this paper and to Alina Chrzastek (University of Wrocław) for ichnological suggestions. Małgorzata Makoś, Paweł Raczyński, Adam Kozłowski and Karol Durkowski are thanked for their support and field assistance. Anna Żylińska kindly verified linguistically the initial version of the manuscript. I thank Stanisław Leszczyński (Jagiellonian University, Kraków) and an anonymous reviewer for their critical reading of an earlier version of the manuscript. Wojciech Nemeč edited and improved the manuscript on behalf of the journal editorial board. The use of LiDAR data in the present study was granted by the academic license no. DIO.DFT.DSI.7211.1619.2015_PL_N issued to the University of Wrocław by the Polish National Head Office of Geodesy and Cartography.

REFERENCES

- Adamovič, J., 1994. Paleogeography of the Jizera Formation (Late Cretaceous sandstones), Kokořín area, central Bohemia. *Sbornik geologických věd*, 46: 103–123.
- Aleksandrowski, P., 1995. The significance of major strike-slip displacements in the development of Variscan structure of the Sudetes (SW Poland). *Przegląd Geologiczny*, 43: 745–754. [In Polish, with English abstract.]
- Allen, J. R. L., 1982. *Sedimentary Structures: Their Character and Physical Basis, Vol. 2. Developments in Sedimentology*, 30B, 643 pp. Elsevier, Amsterdam.
- Andert, H., 1934. Die Fazies in der sudetischen Kreide unter besonderer Berücksichtigung des Elbsandsteingebirges. *Zeitschrift der Deutschen Geologischen Gesellschaft*, 86: 617–637.
- Ashley, G. M., 1990. Classification of large-scale subaqueous bedforms: a new look at an old problem. *Journal of Sedimentary Petrology*, 60: 160–172.
- Awdankiewicz, M., 2006. Fractional crystallization, mafic replenishment and assimilation in crustal magma chambers: geochemical constraints from the Permian post-collisional intermediate-composition volcanic suite of the North-Sudetic Basin (SW Poland). *Geologia Sudetica*, 38: 39–61.
- Badura, J., Pécskay, Z., Koszowska, E., Wolska, A., Zuchiewicz, W. & Przybylski, B., 2006. New data on age and petrological properties of Lower Cenozoic basaltoids, SW Poland. *Przegląd Geologiczny*, 54: 145–153. [In Polish, with English abstract.]
- el Bassyouni, A. A. F. E., 1984. *Sedimentology of the Upper Cretaceous sandstones of the North Sudetic basin in the area between Złotyja, Wleń and Lwówek Śląski*. Ph.D. thesis, University of Wrocław, 170 pp.
- Baranowski, Z., Haydukiewicz, A., Kryza, R., Lorenc, S., Muszyński, A., Solecki, A. & Urbanek, Z., 1990. Outline of the geology of the Góry Kaczawskie (Sudetes, Poland). *Neues Jahrbuch für Geologie und Paläontologie*, 179: 223–257.
- Belderson, R. H., Johnson, M. A. & Kenyon, N. H., 1982. Bedforms. In: Stride, A. H. (ed.), *Offshore Tidal Sands, Process and Deposits*. Chapman & Hall, London, pp. 27–57.
- Berg, G. & Dathe F., 1905/1906. *Geologische Karte von Preußen und benachbarten Bundesstaaten. Blatt Schömburg 1:25 000*. Königliche Geologischen Landesanstalt, Berlin.
- Berg, G. & Dathe, F., 1940. *Geologische Karte des Deutschen Reiches. Blatt Landeshut 1:25 000*. Reichsstelle für Bodenforschung, Berlin.
- Biernacka, J., 2012. Provenance of Upper Cretaceous quartz-rich sandstones from the North Sudetic Synclinorium, SW Poland: constraints from detrital tourmaline. *Geological Quarterly*, 56: 315–332.
- Biernacka, J. & Józefiak, M., 2009. The Eastern Sudetic Island in the Early-to-Middle Turonian: evidence from heavy minerals in the Jerzmanice sandstones, SW Poland. *Acta Geologica Polonica*, 59: 545–565.
- Chrzastek, A. & Wypych, M., 2019. Coniacian sandstones from the North Sudetic Synclinorium revisited: palaeoenvironmental and palaeogeographical reconstructions based on trace fossil analysis and associated body fossils. *Geologos*, 24: 29–53.
- Clifton, H. E., 2005. Coastal sedimentary facies. In: Schwartz, M. L. (ed.), *Encyclopedia of Coastal Science*. Springer-Verlag, Dordrecht, Netherlands, pp. 270–278.
- Collinson, J. & Mountney, N., 2019. *Sedimentary Structures. Fourth edition*. Academic Press Ltd, Dunedin, 340 pp.
- Cymerman, Z., 2004. *Tectonic Map of the Sudetes and the Fore-Sudetic Block, 1:200 000*. Państwowy Instytut Geologiczny, Warszawa.
- Cymerman, Z., 2016. On the need to develop the second edition of the Detailed Geological Map of the Sudetes at the scale of 1:25 000 – current state analysis and assumptions of a comprehensive program for the second edition. *Przegląd*

- Geologiczny*, 64: 604–610. [In Polish, with English abstract.]
- Čech, S., 2011. Palaeogeography and Stratigraphy of the Bohemian Cretaceous Basin (Czech Republic) – an overview. *Geologické výzkumy na Moravě a ve Slezsku*, 1: 18–21.
- Čech, S., Klein, V., Kříž, J. & Valečka, J., 1980. Revision of the Upper Cretaceous stratigraphy of the Bohemian Cretaceous Basin. *Věstník Ústředního ústavu geologického*, 55: 277–296.
- Dalrymple, R. W., 1984. Morphology and internal structure of sandwaves in the Bay of Fundy. *Sedimentology*, 31: 365–382.
- Danišík, M., Migoń, P., Kuhlemann, J., Evans, N. J., Dunkl, I. & Frisch, W., 2010. Thermochronological constraints on the long-term erosional history of the Karkonosze Mts., Central Europe. *Geomorphology*, 117: 78–89.
- Davis, R. A., 2012. Tidal signatures and their preservation potential in stratigraphic sequences. In: Davis, R. A. & Dalrymple, R. W. (eds), *Principles of Tidal Sedimentology*. Springer-Verlag, New York, pp. 35–56.
- Dercourt, J., Gaetani, M., Vrielynck, B., Barrier, E., Biju-Duval, B., Brunet, M. F., Cadet, J. P., Crasquin, S. & Snadulescu, M., 2000. *Atlas Peri-Tethys, Palaeogeographical Maps*. CCGM/CGMW, Paris: 24 maps and explanatory notes: I–XX, 269 pp.
- Don, J., Jerzykiewicz, T., Teisseyre, A. K. & Wojciechowska, I., 1981a. *Szczegółowa Mapa Geologiczna Sudetów. Arkusz Lubawka 1:25 000*. Wydawnictwa Geologiczne, Warszawa. [In Polish.]
- Don, J., Jerzykiewicz, T., Teisseyre, A. K. & Wojciechowska, I., 1981b. *Objaśnienia do Szczegółowej Mapy Geologicznej Sudetów. Arkusz Lubawka 1:25 000*. Wydawnictwa Geologiczne, Warszawa, 89 pp. [In Polish.]
- Dott, R. H. & Bourgeois, J., 1982. Hummocky stratification: significance of its variable bedding sequences. *Geological Society of America Bulletin*, 93: 663–680.
- Dvořák, J., 1968. Stratigrafie, litologie a podloží svrchní křídý ve vnitrosudetické pánvi. *Věstník Českého geologického ústavu*, 43: 423–430. [In Czechish.]
- Dziedzic, K., 1961. Lower Permian of the Intra Sudetic Basin. *Studia Geologica Polonica*, 6: 1–121. [In Polish, with English summary.]
- Flegel, K., 1904. Heuscheuer und Adersbach-Weckelsdorf. Eine Studie über die obere Kreide im böhmisch-schlesischen Gebirge. *Jahres-Bericht Schlesischen der Gesellschaft für vaterländische Kultur*, 82: 114–144.
- Gierwielaniec, J., 1998. Zarys tektoniki i hydrogeologii rowu Wlenia (Sudety Zachodnie). *Górnictwo Odkrywkowe*, 40: 96–127. [In Polish, with English summary.]
- Gorczyca-Skała, J., 1977. Geologic structure of the Wleń Graben. *Geologia Sudetica*, 12: 71–100. [In Polish, with English summary.]
- Harms, J. C., Southard, J. B., Spearing, D. R. & Walker, R. G., 1975. *Depositional Environments as Interpreted from Primary Sedimentary Structures and Stratification Sequences*. Society of Economic Paleontologists and Mineralogists (SEPM), Short Course 2, 161 pp.
- Haq, B. U., 2014. Cretaceous eustasy revisited. *Global and Planetary Change*, 113: 44–58.
- Jerzykiewicz, T., 1968. Sedimentation of the youngest sandstones of the Intrasudetic Cretaceous Basin. *Geologia Sudetica*, 4: 409–462. [In Polish, with English summary.]
- Jerzykiewicz, T., 1969. The brachysyncline of Krzeszow as a tectonic unit (Middle Sudetes). *Bulletin de l'Académie Polonaise des Sciences, Série des Sciences Géologiques et Géographiques*, 17: 37–41.
- Jerzykiewicz, T., 1971. Cretaceous in the vicinity of Krzeszów. *Geologia Sudetica*, 5: 281–318. [In Polish, with English summary.]
- Jerzykiewicz, T. & Wojewoda, J., 1986. The Radków and Szczeliniec sandstones: an example of giant foresets on a tectonically controlled shelf of the Bohemian Cretaceous Basin (Central Europe). In: Knight, R. J. & McLean, J. R. (eds), *Shelf Sands and Sandstones*. Canadian Society of Petroleum Geologists, Memoir, 11: 1–15.
- Johnson, H. D. & Baldwin, C. T., 1996. Shallow clastic seas. In: Reading, H. G. (ed.), *Sedimentary Environments: Processes, Facies and Stratigraphy*. Blackwell Publishing, Oxford, pp. 232–280.
- Kolb, W., 1936. Tektonische Untersuchungen im Gebiet des Lähner Grabens. *Jahrbuch der Preußischen Geologischen Landesanstalt*, 56: 93–124.
- Kowalski, A., 2015. *Geological map of the Różana-Łączna area with particular focus on sedimentary rocks and use of LiDAR data*. Master thesis, University of Wrocław, Wrocław, 107 pp.
- Kowalski, A., 2016. Granica trias-kreda na obszarze brachysynkliny Krzeszowa i elewacji Łącznej (synklinorium śród-sudeckie). In: Olszewska-Nejbert, D., Filipek, A., Bąbel, M. & Wysocka, A. (eds), *Abstrakty, VI Polska Konferencja Sedymentologiczna POKOS 6: Granice Sedymentologii*. Uniwersytet Warszawski, Warszawa, pp. 161–162. [In Polish.]
- Kowalski, A., 2017. Fault geometry and evidence of depocentre migration within a transtensional intra-basinal high – a case study from the Łączna Anticline (Intrasudetic Synclinorium, SW Poland). *Geological Quarterly*, 61: 779–794
- Kowalski, A., 2018. Landslides and the incorrect interpretation of geological structure – examples from the Sudety Mountains. *Biuletyn Państwowego Instytutu Geologicznego*, 473: 27–148. [In Polish, with English summary.]
- Kowalski, A., 2020a. Triassic palaeogeography of NE Bohemian Massif based on sedimentological record in the Wleń Graben and the Krzeszów Brachysyncline (SW Poland). *Annales Societatis Geologorum Poloniae*, 90: 125–148.
- Kowalski, A., 2020b. Multistage structural evolution of the end-Cretaceous–Cenozoic Wleń Graben (the Sudetes, NE Bohemian Massif) – a contribution to the post-Variscan tectonic history of SW Poland. *Annales Societatis Geologorum Poloniae*, 90 (in press): doi: <https://doi.org/10.14241/asgp.2020.21>.
- Kowalski, A., Durkowski, K. & Raczynski, P., 2018. Zechstein marine deposits in the Wleń Graben (North Sudetic Synclinorium, SW Poland) – new insights into the palaeogeography of the southern part of the Polish Zechstein Basin. *Annales Societatis Geologorum Poloniae*, 88: 321–339.
- Kozłowski, S. & Parachoniak, W., 1967. Wulkanizm permski w depresji północnosudeckiej. *Prace Muzeum Ziemi*, 11: 191–221. [In Polish.]
- Leszczyński, S., 2010. Coniacian–?Santonian paralic sedimentation in the Rakowice Małe area of the North Sudetic Basin, SW Poland: sedimentary facies, ichnological record and palaeogeographical reconstruction of an evolving marine embayment. *Annales Societatis Geologorum Poloniae*, 80: 1–24.

- Leszczyński, S., 2018. Integrated sedimentological and ichnological study of the Coniacian sedimentation in North Sudetic Basin, SW Poland. *Geological Quarterly*, 62: 767–816.
- Leszczyński, S. & Nemeč, W., 2020. Sedimentation in a synclinal shallow-marine embayment: Coniacian of the North Sudetic Synclinorium, SW Poland. *The Depositional Record*, 6: 144–171.
- Longhitano, S. G., 2013. A facies-based depositional model for ancient and modern, tectonically-confined tidal straits. *Terra Nova*, 25: 446–452.
- Longhitano, S. G. & Nemeč, W., 2005. Statistical analysis of bed thickness variation in a Tortonian succession of biocalcarenitic tidal dunes, Amantea Basin, Calabria, southern Italy. *Sedimentary Geology*, 179: 195–224.
- Malkovský, M., 1987. The Mesozoic and Tertiary basins of the Bohemian Massif and their evolution. *Tectonophysics*, 137: 31–42.
- Miall, A. D., 1978. Lithofacies types and vertical profile models in braided river deposits: a summary. In: Miall, A. D. (ed.), *Fluvial Sedimentology*. Canadian Society of Petroleum Geologists, Memoir, 5: 597–604.
- Miall, A. D., 1985. Architectural element analysis: a new method of facies analysis applied to fluvial deposits. *Earth-Science Reviews*, 22: 261–308.
- Milewicz, J., 1959. Notes on the tectonics of Lwówek Śląski (Lower Silesia). *Kwartalnik Geologiczny*, 3: 1024–1032. [In Polish, with English summary.]
- Milewicz, J., 1965. Rotliegende deposits in the vicinity of Lwówek Śląski. *Biuletyn Instytutu Geologicznego*, 185, *Z badań geologicznych na Dolnym Śląsku*, 11: 195–217. [In Polish, with English summary.]
- Milewicz, J., 1966. The Zechstein of the Wleń Graben. *Kwartalnik Geologiczny*, 10: 63–73. [In Polish, with English summary.]
- Milewicz, J., 1968a. The Geological structure of the North-Sudetic Depression. *Biuletyn Instytutu Geologicznego*, 227, *Z badań geologicznych na Dolnym Śląsku*, 17: 5–31.
- Milewicz, J., 1968b. On the Buntsandstein deposits in the Lwówek Graben and in the adjacent areas. *Kwartalnik Geologiczny*, 12: 547–560. [In Polish, with English summary.]
- Milewicz, J., 1985. A proposal of formal stratigraphic subdivision of the infill of the North Sudetic Depression. *Przegląd Geologiczny*, 33: 385–389. [In Polish, with English summary.]
- Milewicz, J., 1997. Upper Cretaceous of the North Sudetic depression. Litho- and biostratigraphy, tectonics and remarks on raw materials. *Acta Universitatis Wratislaviensis, Prace Geologiczno-Mineralogiczne*, 61: 1–58. [In Polish, with English summary.]
- Milewicz, 2006. O osadach santonickich na obszarze basenu północnosudeckiego. *Przegląd Geologiczny*, 54: 693–694. [In Polish.]
- Milewicz, J. & Frąckiewicz, W., 1983. *Szczegółowa Mapa Geologiczna Sudetów. Arkusz Wleń 1:25 000*. Wydawnictwa Geologiczne, Warszawa. [In Polish.]
- Milewicz, J. & Frąckiewicz, W., 1988. *Objaśnienia do Szczegółowej Mapy Geologicznej Sudetów. Arkusz Wleń 1:25 000*. Wydawnictwa Geologiczne, Warszawa, 75 pp. [In Polish.]
- Mitchell, A. J., Uličný, D., Hampson, G. J., Allison, P. A., Gorman, G. J., Piggott, M. D., Wells, M. R. & Pain, C. C., 2014. Modelling tidal current-induced bed shear stress and palaeocirculation in an epicontinental seaway: the Bohemian Cretaceous Basin, Central Europe. *Sedimentology*, 57: 359–388.
- Mroczkowski, J., 1969. Palaeocurrents in the Lower Triassic Deposits of the southern part of the Northsudetic Basin. *Bulletin de l'Académie Polonaise des Sciences, Serie des Sciences Geologiques et Geographiques*, 17: 167–172.
- Mroczkowski, J., 1972. Sedimentation of the Bunter in the Northsudetic Basin. *Acta Geologica Polonica*, 22: 351–377. [In Polish, with English summary.]
- Mroczkowski, J., 1977. Lower Triassic sandstones in the northern part of the Intra-Sudetic trough. *Annales Societatis Geologorum Poloniae*, 47: 49–72. [In Polish, with English summary.]
- Mroczkowski, J. & Mader, D., 1985. Sandy inland braidplain deposition with local aeolian sedimentation in the Lower and Middle parts of the Buntsandstein and sandy coastal braidplain deposition in the topmost Zechstein in the Sudetes (Lower Silesia, Poland). In: Mader, D. (ed.), *Aspects of Fluvial Sedimentation in the Lower Triassic Buntsandstein of Europe. Lecture Notes in Earth Sciences*, 4: 165–195. Springer-Verlag, Berlin.
- Nádaskay, R. & Uličný, D., 2014. Genetic stratigraphy of Coniacian deltaic deposits of the northwestern part of the Bohemian Cretaceous Basin. *Zeitschrift der Deutschen Gesellschaft für Geowissenschaften*, 165: 547–575.
- Nádaskay, R., Kochergina, Y. V., Čech, S., Švábenická, L., Valečka, J., Erban, V., Halodová, P. & Čejková, B., 2019. Integrated stratigraphy of an offshore succession influenced by intense siliciclastic supply: implications for Coniacian tectono-sedimentary evolution of the West Sudetic area (NW Bohemian Cretaceous Basin, Czech Republic). *Cretaceous Research*, 102: 127–159.
- Nemeč, W., Porębski S. & Teisseyre, A. K., 1982. Explanatory notes to the lithotectonic molasse profile of the Intra-Sudetic Basin, Polish Part (Sudety Mts., Carboniferous-Permian). *Veröffentlichung des Zentralinstituts für Physik der Erde AdW DDR, Potsdam*, 66: 267–277.
- Niebuhr, B., 2019. From animal to plant kingdom: the alleged sponge *Siphonia bovista* Geinitz from the Cretaceous of Saxony (Germany) in fact represents internal moulds of the cone-like plant fossil *Dammarites albens* Presl in Sternberg. *Bulletin of Geosciences*, 94: 221–234.
- Partsch, J., 1896. *Schlesien. Eine Landeskunde für das deutsche Volk, 1. Teil: Das ganze Land*. Ferdinand Hirt, Breslau, 420 pp.
- Peryt, T., 1978. Outline of the Zechstein stratigraphy in the North Sudetic Trough. *Kwartalnik Geologiczny*, 22: 59–82. [In Polish, with English summary.]
- Potter, P. E. & Pettijohn, F. J., 1963. *Palaeocurrents and Basin Analysis*. Springer-Verlag, Berlin, 296 pp.
- Prouza, V., Tásler, R. & Valin, F., 1985. Gravelly to sandy braidplain deposition in the Buntsandstein-facies Bohdašín Formation in northeastern Bohemia. In: Mader, D. (ed.), *Aspects of Fluvial Sedimentation in the Lower Triassic Buntsandstein of Europe. Lecture Notes in Earth Sciences*, 4: 397–410. Springer-Verlag, Berlin.
- Raczyński, P., 1997. Depositional conditions and paleoenvironments of the Zechstein deposits in the North-Sudetic Basin (SW Poland). *Przegląd Geologiczny*, 45: 693–699. [In Polish, with English summary.]

- Raczyński, P., Kurowski, L. & Mastalerz, K., 1998. Litostratygrafia i ewolucja basenu północnosudeckiego na przełomie paleozoiku i mezozoiku. In: Wojewoda, J. (ed.), *Ekologiczne Aspekty Sedymentologii. Tom 1. Materiały VII Krajowego Spotkania Sedymentologów, Wojcieszów 2-4 lipca 1998 r.* WIND, Wrocław, pp. 75–100. [In Polish.]
- Radwański, S., 1975. Upper Cretaceous of the Central Part of the Sudetes in the light of new borehole materials. *Biuletyn Instytutu Geologicznego*, 287, *Z badań geologicznych na Dolnym Śląsku*, 24: 5–59. [In Polish, with English summary.]
- Raumer, K., 1819. *Das Gebirge Nieder-Schlesiens, der Grafschaft Glatz und eines Theils von Böhmen und der Ober-Lausitz geognostisch dargestellt (XVI)*. G. Reimer, Berlin, 182 pp.
- Reading, H. G. & Collinson, J. D., 1996. Clastic coasts. In: Reading, H. G. (ed.), *Sedimentary Environments: Processes, Facies and Stratigraphy*. Blackwell Publishing, Oxford, pp. 154–231.
- Rotnicka, J., 2005. Ichnofabrics of the Upper Cretaceous fine-grained rocks from the Stołowe Mountains (Sudetes, SW Poland). *Geological Quarterly*, 49: 15–30.
- Sawicki, L., 1995. *Geological Map of Lower Silesia with Adjacent Czech and German Territories (without Quaternary Deposits)*. Państwowy Instytut Geologiczny, Warszawa.
- Scupin, H., 1910. Über sudetische prätertiäre junge Krustenbewegungen und die Verteilung von Wasser und Land zur Kreidezeit in der Umgebung der Sudeten und des Erzgebirges. *Zeitschrift für Naturwissenschaften*, 82: 321–344.
- Scupin, H., 1913. Die Löwenberger Kreide und ihre Fauna. *Palaeontographica – Supplement* 6: 1–275.
- Scupin, H., 1933. Der Buntsandstein der Nordsudeten. *Zeitschrift der Deutschen Geologischen Gesellschaft*, 85: 161–189.
- Scupin, H., 1935. Die stratigraphischen Beziehungen der mittel- und nordsudetischen Kreide. *Zeitschrift der Deutschen Geologischen Gesellschaft*, 87: 523–538.
- Scupin, H., 1936. Zur Paläogeographie des sudetischen Kreidemeeres. *Zeitschrift der Deutschen Geologischen Gesellschaft*, 88: 309–325.
- Skoček, V. & Valečka, J., 1983. Paleogeography of the Late Cretaceous Quadersandstein of Central Europe. *Palaeogeography, Palaeoclimatology, Palaeoecology*, 44: 71–92.
- Śliwiński, W., 1980. A model for caliche formation in the continental Permian deposits of southwestern Intra-Sudetic Basin, southwestern Poland. *Geologia Sudetica*, 15: 83–101.
- Śliwiński, W., 1981. Dolomites in the Chelmsko Śląskie Beds (Permian, Intra-Sudetic Basin), a reminiscence of the Permian volcanism. In: Dziedzic, K. (ed.), *Problems of Hercynian Volcanism in Central Sudetes*. Wydawnictwo Uniwersytetu Wrocławskiego, Wrocław, pp. 106–110. [In Polish, with English summary.]
- Śliwiński, W., 1984. Proposed revision of the stratigraphic position of Chelmsko Śląskie Beds (Permian, Intra-Sudetic Basin). *Geologia Sudetica*, 18: 167–174. [in Polish with English summary.]
- Śliwiński, W., Raczyński, P. & Wojewoda, J., 2003. Sedymentacja utworów epiwaryscyjskiej pokrywy osadowej w basenie północnosudeckim. In: Ciężkowski, W., Wojewoda, J. & Żelaźniewicz, A. (eds), *Sudety Zachodnie: od wendy do czwartorzędu*. WIND, Wrocław, pp. 119–126. [In Polish.]
- Solecki, A., 1994. Tectonics of the North Sudetic Synclinorium. *Acta Universitatis Wratislaviensis, Prace Geologiczno-Mineralogiczne*, 65: 1–38.
- Solecki, A., 2011. Structural development of the epi-Variscan cover in the North Sudetic Synclinorium area. In: Żelaźniewicz, A., Wojewoda, J. & Ciężkowski, W. (eds), *Mezozoik i Kenozoik Dolnego Śląska*. WIND, Wrocław, pp. 19–36. [In Polish, with English abstract.]
- Stroga, C., Bobiński, W. & Kozdrój, W., 2018. Geological setting of the barite-fluorite deposit at Jeżów Sudecki (Kaczawa Mts.). *Biuletyn Państwowego Instytutu Geologicznego*, 472: 231–254. [In Polish, with English summary.]
- SPDPSH (System Przetwarzania Danych Państwowej Służby Hydrogeologicznej), 2019. *Centralny Bank Danych Hydrogeologicznych*. <https://www.pgi.gov.pl/psh/dane-hydrogeologiczne-psh/947-bazy-danych-hydrogeologiczne/9057-bankhydro.html>, accessed: 10-06-2019. [In Polish.]
- Szałamacha, J. & Szałamacha, M., 1993a. *Szczegółowa Mapa Geologiczna Sudetów. Arkusz Dziwiszów 1:25 000*. Polish Geological Institute, Warszawa. [In Polish.]
- Szałamacha, J. & Szałamacha, M., 1993b. *Objaśnienia do Szczegółowej Mapy Geologicznej Sudetów. Arkusz Dziwiszów 1:25 000*. Wydawnictwa Geologiczne, Warszawa, 43 pp. [In Polish.]
- Tásler, R., 1964. Permokarbon vnitrosudetické pánve a podkrkonošské pánve. In: Svoboda, J. (ed), *Regionální geologie ČSSR. Díl I, Český masív, sv. 2. Algonkium až kvartér*. Ústřední ústav geologický, Praha, pp. 204–232. [In Czechish.]
- Teisseyre, B., 1972. Lower Turonian microfauna from Krzeszów (Sudetes). *Acta Geologica Polonica*, 22: 71–81.
- Turnau, E., Żelaźniewicz, A. & Franke, W., 2002. Middle to early late Viséan onset of late orogenic sedimentation in the Intra-Sudetic Basin, West Sudetes: miopore evidence and tectonic implication. *Geologia Sudetica*, 34: 9–16.
- Uličný, D., 2001. Depositional systems and sequence stratigraphy of coarse-grained deltas in a shallow-marine, strike-slip setting: the Bohemian Cretaceous Basin, Czech Republic. *Sedimentology*, 48: 599–628.
- Uličný, D., 2004. A drying-upward aeolian system of the Bohdašín Formation (Early Triassic), Sudetes of NE Czech Republic: record of seasonality and long-term palaeoclimate change. *Sedimentary Geology*, 167: 17–39.
- Uličný, D., Laurin J. & Čech, S., 2009a. Controls on clastic sequence geometries in a shallow-marine, transtensional basin: the Bohemian Cretaceous Basin, Czech Republic. *Sedimentology*, 56: 1077–1114.
- Uličný, D., Špičáková, L., Grygar, R., Svobodová, M., Čech, S. & Laurin J., 2009b. Palaeodrainage systems at the basal unconformity of the Bohemian Cretaceous Basin: roles of inherited fault systems and basement lithology during the onset of basin filling. *Bulletin of Geosciences*, 84: 577–610.
- Valečka, J., 1984. Storm surge versus turbidite origin of the Coniacian to Santonian sediments in the eastern part of the Bohemian Cretaceous Basin. *Geologische Rundschau*, 73: 651–682.
- Vejbæk, O. V., Andersen, C., Duser, M., Herngreen, W., Krabbe, H., Leszczyński, K., Lott, G. K., Mutterlose, J. & van der Molen, A. S., 2010. Cretaceous. In: Doornenbal, J. C. & Stevenson, A. G. (eds), *Petroleum Geological Atlas of*

- the Southern Permian Basin Area*. EAGE Publications b.v., Houten, pp. 195–209.
- Voigt, S., Wagreeich, M., Surlyk, H., Walaszczyk, I., Uličný, D., Čech, S., Voight, T., Wiese, F., Wilmsen, M., Niebuhr, B., Reich, M., Funk, H., Michalík, J., Jagt, J. W. M., Felder, P. J. & Schulp, A. S., 2008. Cretaceous. In: McCann, T. (ed.), *The Geology of Central Europe*. The Geological Society, London, pp. 923–997.
- Wilmsen, M., Uličný, D. & Košťák, M., 2014. Cretaceous basins of Central Europe: deciphering effects of global and regional processes – a short introduction. *Zeitschrift der Deutschen Gesellschaft für Geowissenschaften*, 165: 495–499.
- Wojewoda, J., 1997. Upper Cretaceous littoral-to-shelf succession in the Intrasudetic Basin and Nysa Trough, Sudety Mts. In: Wojewoda, J. (ed.), *Obszary Źródłowe: Zapis w Osadach*, 1: 81–96. WIND, Wrocław.
- Wojewoda, J., 1998a. Geologia, litostratygrafia i warunki sedymentacji kredy. In: Wojewoda, J. (ed.), *Ekologiczne aspekty sedymentologii. Tom 1. Materiały VII Krajowego Spotkania Sedymentologów, Wojcieszów, Poland, July 2–4, 1998*. WIND, Wrocław, pp. 54–58. [In Polish.]
- Wojewoda, J., 1998b. Opis stanowisk terenowych. Stanowisko 5 (Gorzszowskie Skały). In: Wojewoda, J. (ed.), *Ekologiczne aspekty sedymentologii. Tom 1. Materiały VII Krajowego Spotkania Sedymentologów, Wojcieszów, Poland, July 2–4, 1998*. WIND, Wrocław, pp. 70–71. [In Polish.]
- Wojewoda, J., 1998c. Opis stanowisk terenowych. Stanowisko 6 (Krzeszówek). In: Wojewoda, J. (ed.), *Ekologiczne aspekty sedymentologii. Tom 1. Materiały VII Krajowego Spotkania Sedymentologów, Wojcieszów, Poland, July 2–4, 1998*. WIND, Wrocław, pp. 72. [In Polish.]
- Wojewoda, J., 2003. “Gilbert Type Delta” versus “Accumulation Terraces” models and their application to middle Turonian-early Coniacian sedimentary setting in the Intrasudetic Basin: A discussion. *Geolines*, 16: 109–110.
- Wojewoda, J., 2007. Neotectonic aspect of the Intrasudetic Shear Zone. *Acta Geodynamica et Geomaterialia*, 4: 31–41.
- Wojewoda, J., 2016. About the need to develop the second edition of the detailed geological map of the Sudetes at the scale of 1:25 000 – examples of a revision of the geological pattern using the LiDAR Digital Elevation Models. *Przegląd Geologiczny*, 64: 597–603. [In Polish, with English abstract.]
- Wojewoda, J. & Mastalerz, K., 1989. Climate evolution, allo- and autocyclicity of sedimentation: an example from the Permo-Carboniferous continental deposits of the Sudetes, SW Poland. *Przegląd Geologiczny*, 37: 173–180. [In Polish, with English summary.]
- Wojewoda J., Rauch, M. & Kowalski A., 2016. Synsedimentary seismotectonic features in Triassic and Cretaceous sediments of the Intrasudetic Basin (U Deviti křižů locality) – regional implications. *Geological Quarterly*, 60: 355–364.
- Wojtkowiak, A., Zawistowski, K., Ihnatowicz, A. & Biel, A., 2009. *Dokumentacja geologiczna inna z wykonania hydrogeologicznych otworów badawczych dla projektowanej stacji hydrogeologicznej I rzędu w Dobromyślu*. Unpublished report. Centralne Archiwum Geologiczne, Państwowy Instytut Geologiczny – Państwowy Instytut Badawczy, Warszawa, 27 pp. [In Polish.]
- Żelaźniewicz, A., Aleksandrowski, P., Buła, Z., Karnkowski P. H., Konon, A., Oszczytko, N., Ślącza, A., Zaba, J. & Żytko, K., 2011. *Regionalizacja Tektoniczna Polski*. Komitet Nauk Geologicznych Polskiej Akademii Nauk, Wrocław, 60 pp. [In Polish.]
- Ziegler, P. A., 1990. *Geological Atlas of Western and Central Europe*. Shell International Petroleum Maatschappij B.V., Rijsvijk, 239 pp.
- Zieliński, T. & Pisarska-Jamroży, M., 2012. Which features of deposits should be included in a code and which not? *Przegląd Geologiczny*, 60: 387–397. [In Polish, with English abstract.]
- Zimmermann, E., 1932. *Geologische Karte von Preussen und benachbarten deutschen Ländern. Lieferung 276, Blatt Hirschberg 1:25 000*. Preußische Geologische Landesanstalt, Berlin.
- Ziółkowska, M., 1990. Glauconite from the Upper Cretaceous deposits of the Inner Sudetic Depression. *Przegląd Geologiczny*, 38: 433–437. [In Polish, with English summary.]